SYNTHESIS AND CHARACTERIZATIONS OF MAGNETIC CARBON SAND

Yattiphong Kaeokhamchan

A Thesis Submitted in Partial Fulfillment of the Requirement for the

Degree of Master of Science in Physics

Suranaree University of Technology

Academic Year 2019

การสังเคราะห์และศึกษาลักษณะของฟิล์มแม่เหล็กคาร์บอนบนทราย

นายญัดติพงษ์ แก้วคำจันทร์

มหาวิทยาลัยเทคโนโลยีสุรนารี

วิทยานิพนธ์นี้เป็นส่วนหนึ่งของการศึกษาตามหลักสูตรปริญญาวิทยาศาสตรมหาบัณฑิต
สาขาวิชาฟิสิกส์
มหาวิทยาลัยเทคโนโลยีสุรนารี
ปีการศึกษา 2562

SYNTHESIS AND CHARACTERIZATIONS OF MAGNETIC CARBON SAND

Suranaree University of Technology has approved this thesis submitted in partial fulfillment of the requirements for a Master's degree.

Thesis Examining Committee

(Assoc. Prof. Dr. Panomsak Meemon)
Chairperson

(Assoc. Prof. Dr. Worawat Meevasana)
Member (Thesis Advisor)

(Dr. Wiwat Nuansing)
Member

(Assoc. Prof. Dr. Supree Pinitsoontorn)
Member

(Assoc. Prof. Flt. Lt. Dr. Kontorn Chamniprasart)
Vice Rector for Academic Affairs and Internationalization

(Assoc. Prof. Dr. Worawat Meevasana)
Dean of Institute of Science

มหาวิทยาลัยเทคโนโลยีสุรนารี

ณัดติพงษ์ แก้วคำจันทร์ : การสังเคราะห์และศึกษาลักษณะของฟิล์มแม่เหล็กคาร์บอนบนทราย (SYNTHESIS AND CHARACTERIZATIONS OF MAGNETIC CARBON SAND). อาจารย์ที่ปรึกษา : รองศาสตราจารย์ ดร.วรวัฒน์ มีวาสนา, 52 หน้า.

ในการศึกษาครั้งนี้ ฟิล์มแม่เหล็กคาร์บอนบนทรายถูกเตรียมโดยวิธีการเคลือบด้วยไอเคมี (Chemical vapor deposition) ซึ่งใช้สารตั้งต้นในการเตรียมฟิล์มคืออะดาเมนเทน (adamantane) อะดาเมนเทนเป็นโมเลกุลที่เล็กที่สุดของวัสดุที่เป็นไฮโดรคาร์บอนที่มีโครงสร้างคล้ายเพชรที่เรียกว่าไดมอนดรอยด์ สารตั้งต้นอะดาเมนเทนถูกทำให้ระเหยจากนั้นปล่อยให้เคลือบลงบนทรายที่อุณหภูมิประมาณ 1,050 องศาเซลเซียส จากการวัดคุณสมบัติแม่เหล็กของฟิล์มแม่เหล็กคาร์บอนบนทรายแสดงให้เห็นถึงลักษณะฮีสเตอรีซีสซึ่งแสดงถึงคุณสมบัติเฟอร์โรแมกเนติก ค่าอิ่มตัวแมกนีไตเซชันวัดที่อุณหภูมิห้องมีค่าประมาณ 72 m-emu/g โดยผลการวิเคราะห์องค์ประกอบของธาตุด้วย Energy dispersive x-ray spectroscopy (EDS) พบว่าไม่มีการปนเปื้อนขององค์ประกอบของวัสดุแม่เหล็ก เช่น นิกเกิล โคบอลต์ และเหล็ก ในคาร์บอนฟิล์มของเรา จากผลรามานสเปกตรัมแสดงให้เห็นถึงการเปลี่ยนแปลงโครงสร้างของอะดาเมนเทนหลังจากผ่านกระบวนเคลือบด้วยไอเคมี จากนั้นเราได้ทำการศึกษาคุณสมบัติเฟอร์โรแมกเนติกในฟิล์มคาร์บอนของเรานี้ ซึ่งอาจจะเกิดขึ้นเนื่องจากอิเล็กตรอนโดดเดี่ยวที่เกิดขึ้นในฟิล์ม ตัวอย่างเช่น พันธะคาร์บอนที่ไม่สมบูรณ์ หรือที่เรียกว่า Carbon dangling bond ซึ่งเป็นผลมาจากการเผาอะดาเมนเทนที่อุณหภูมิสูง โดยการศึกษาด้วยการทดสอบลดค่าความอิ่มตัวของแม่เหล็กในคาร์บอนฟิล์มของเราด้วยการสัมผัสกับความชื้นโดยใช้การต้มในน้ำเพื่อเร่งการเกาะติดระหว่างน้ำและพันธะคาร์บอนที่ไม่สมบูรณ์ในคาร์บอนฟิล์มของเรา ซึ่งค่าอิ่มตัวแมกนีไตเซชันมีการลดลงเหลือ 53 m-emu/g การลดลงของค่าอิ่มตัวแมกนีไตเซชันนี้เกิดจากการลดลงของอิเล็กตรอนโดดเดี่ยวหรือพันธะคาร์บอนที่ไม่สมบูรณ์เนื่องจากการยึดเกาะกับโมเลกุลของน้ำ ซึ่งถูกยืนยันโดยผลของรามานสเปกตรัมที่แสดงให้เห็นถึงพีคที่เป็นคุณสมบัติของน้ำ นอกจากนี้การต้มและการอบภายใต้บรรยากาศแก๊สอาร์กอนยังส่งผลต่ออัตราส่วนระหว่างพื้นที่ของ G พีค และ D พีคด้วย การเปลี่ยนแปลงของอัตราส่วนนี้เกี่ยวข้องกับการเปลี่ยนแปลงค่าอิ่มตัวแม่เหล็กและสนับสนุนสมมติฐานของเราที่ว่าความเป็นแม่เหล็กเฟอโรในคาร์บอนฟิล์มของเราอาจจะเกิดขึ้นเนื่องจากพันธะคาร์บอนที่ไม่สมบูรณ์ งานวิจัยนี้น่าจะเป็นประโยชน์ในการเตรียมวัสดุคาร์บอนแม่เหล็กด้วยกระบวนการที่ราคาไม่สูง

สาขาวิชาฟิสิกส์ ลายมือชื่อนักศึกษา ณัดติพงษ์ แก้วคำจันทร์

ปีการศึกษา 2562 ลายมือชื่ออาจารย์ที่ปรึกษา

YATTIPHONG KAEOKHAMCHAN : SYNTHESIS AND CHARACTERIZATIONS OF MAGNETIC CARBON SAND. THESIS ADVISOR : ASSOC. PROF. WORAWAT MEEVASANA, Ph.D. 52 PP.

ADAMANTANE/ DIAMONDIODE/ FERROMAGNETISM/ DANGGLING BOND/ CHEMICAL VAPOR DEPORSITION

In this work, the magnetic carbon sand (MCS) has been successfully prepared by the chemical vapor deposition (CVD) using adamantane ($C_{10}H_{16}$) as a precursor. The MCS was obtained by the deposition of adamantane precursor at 1050 °C. The magnetization of MCS was measured by the vibrating sample magnetometer (VSM) with applied magnetic field in the range between -15 and 15 kOe. From the VSM results, the magnetic hysteresis loops were observed to show ferromagnetic behavior where energy dispersive x-ray measurement (EDS) showed no contamination of the common magnetic elements (i.e. Ni, Co, Fe) in our MCS. The saturated magnetization could be as high as 72 m-emu/g at room temperature. The Raman-spectroscopy measurement shows that the adamantane structure has changed after the CVD process.

We then tested the suggestions from previous studies that the observed ferromagnetism in MCS could come from the unpaired electrons in carbon (i.e. dangling bond) which could occur during the calcination process at high temperature; the test was to see if we could reduce magnetization of MCS by humidity treatment which would promote the bonding between water molecules and the unpaired electrons of MCS. The saturation magnetization of MCS was observed to be decreased from 72 m-emu/g to 53 m-emu/g after the boiling process. The decrease of magnetization could

be described by the saturation of unpaired electrons or dangling bonds where those defects are eliminated when attached to the water; this is confirmed by the Raman spectrum with presence of a water molecule peak at approximately 3651 cm^{-1}. Furthermore, both the boiling process and the annealing-in-Ar process also affect the ratios of G and D peak area (A_G/A_D). This correlates very well with the change of the measured saturated magnetization and hence supports our hypothesis that the ferromagnetism in MCS is caused by the presence of the C-dangling bonds.

Regarding the application, this work suggests an inexpensive method for preparing magnetic carbon particles and also modifying its magnetization.

มหาวิทยาลัยเทคโนโลยีสุรนารี

School of Physics

Academic Year 2019

Student's Signature

Advisor's Signature

ACKNOWLEDGEMENTS

My thesis could not have been completed without many great help and support from many people. First of all, I would like to thank my advisor, Assoc. Prof. Dr. Worawat Meevasana. I appreciate all of his support and encouragement in research works and life skills. Throughout time, studying bachelor degree and master degrees was a great to work experience, I have to learn new aspects of research and good teamwork. I feel like I am very lucky to learn these things with him.

I would like to thank Assoc. Prof. Dr. Supree Pinitsoontorn from the Department of Physics, Khon Kean university, who has kindly taught and support me to operate a vibrating sample magnetometer. Without this help, the magnetic properties of carbon film on sand could not be achieved.

In Meevasana group research, I would like to thank Mr. Suppanut Sangphet who taught me how to prepare adamantane films by CVD technique and gives great help. I would like to thank Dr. Tanachat Eknapakul and Mr. Worasarit Saengsui for useful discussion and assistance throughout the experiment. In addition, I would like to thank all of the members of Meevasana group for always supporting and good relationships.

This work has been partially supported by Suranaree University of Technology and the Research Network NANOTEC (RNN) program of the National Nanotechnology Center (NANOTEC), NSTDA, Ministry of Science and Technology, Thailand. Y. Keaokhamchan acknowledges the Development and Promotion of Science and Technology Talents Project (DPST) scholarship.

Yattiphong Kaeokhanchan

CONTENTS

Page

ABSTRACT IN THAI I

ABSTRACT IN ENGLISH II

ACKNOWLEDGEMENTS IV

CONTENTS V

LIST OF FIGURES VIII

CHAPTER

I INTRODUCTION 1

1.1 Motivation 1

1.2 Research objectives 2

1.3 Magnetic properties 3

1.3.1 Diamagnetism 5

1.3.2 Paramagnetism 5

1.3.3 Ferromagnetism 6

1.3.4 Hysteresis loop 7

1.3 Outline of thesis 8

II REVIEW OF FERROMAGNETISM IN CARBON-BASED MATERALS 10

2.1 Ferromagnetism in carbon-based materials 10

2.1.1 The studies of ferromagnetism in carbon-based materials 10

CONTENTS (Continued)

Page

2.1.2 Origin of ferromagnetism in carbon-based materials 14

2.2 Effect of humidity treatment on ferromagnetism in carbon-based materials 19

2.3 Basic knowledge about diamondoid and adamantane 21

2.3.1 Diamondoid 21

2.3.2 Adamantane 21

2.4 Diamond like carbon 22

III METHODS 24

3.1 Sample preparations: magnetic carbon sand (MCS) 24

3.2 Scanning electron microscopy (SEM) 25

3.3 Energy dispersive X-ray spectroscopy (EDS) 28

3.4 Raman spectroscopy 29

3.5 The vibrating sample magnetometer 31

3.6 Study effect of humidity treatment on MCS's magnetism 32

IV RESULTS AND DISCUSSION 33

4.1 Characterization of the MCS morphology 33

4.1.1 Physical characteristics of MCS 33

4.1.2 Energy dispersive x-ray spectroscopy of MCS 35

4.2 The magnetic property of MCS 37

4.3 Raman spectrum of MCS 38

CONTENTS (Continued)

Page

4.4 Effect of humidity treatment on MCS's magnetism..... 40

V CONCLUSIONS..... 45

5.1 Conclusion of study ferromagnetism in MCS..... 45

5.2 Future direction 46

REFERENCES..... 47

CURRICULUM VITAE..... 52

มหาวิทยาลัยเทคโนโลยีสุรนารี

LIST OF FIGURES

Figure **Page**

1.1 Schematic responding of diamagnetic, paramagnetic, and ferromagnetic materials to the presence of a magnetic field H (edit from Pinitsoontorn, 2015) 4

1.2 Hysteresis loop model of ferromagnetic material 6

1.3 Difference between hysteresis characteristics of hard and soft ferromagnetic material 8

2.1 XRD patterns of (a) polyacrylonitrile powder and (b) carbon material prepared by pyrolysis of polyacrylonitrile at 1273 K for 1 h. The red straight lines show the usual peak positions of the graphite structure (Saito et al., 2011) 12

2.2 Magnetic moment measured at T= 300 K as a function of the magnetic field for highly oriented pyrolytic graphite sample before (□) and after (•) proton irradiation (the background signal was subtracted) (Esquinazi et al., 2003) 12

2.3 (a) Schematic cross-sections of the (left) as-grown and (right) exfoliated regions. After the exfoliation, partially aligned dangling bonds are expected at the surface. (b) Room-temperature magnetization curves, subtracted by diamagnetic background, of as-grown (black), 1st (blue), 2nd (green), 3rd (yellow), and 4th (red) exfoliated CVD-carbon film on a quartz substrate (Sangphet et al., 2018) 13

LIST OF FIGURES (Continued)

Figure **Page**

2.4 Model of (a) antiferromagnetic and (b) ferromagnetic spin configurations of the C60 cage open. (adapted from Kim et al., 2003) 15

2.5 Schematic illustration of (a) carbon chain structure in Teflon tape, (b) - (c) cutting and stretching of a Teflon tape, respectively, (d) - (e) dangling bonds created after cutting, and (f) - (g) carbon dangling bonds formed in Teflon by mechanical stretching. (Ma et al., 2012) 16

2.6 Rh-C_{60} polymer without (a) and with (b) one vacancy per C_{60} unit. The atoms surrounding the vacancy are shown in red, while the sp^3 atoms are shown in green (Andriotis et al., 2003)..... 17

2.7 (a) Structure, charge density (e/(A^3)˙), and (b) spin density (e/(A^3)˙) of the graphite vacancy. Density plots are slices in the graphene plane (Lehtinen et al., 2004) 18

2.8 Models atomic structures of a CNT containing a reconstructed monovacancy (a) - (b), divacancy (c) - (d), and trivacancy (e) - (f) in various topological orientations. The newly formed carbon bonds (red sticks) and the dangling carbon atoms (red balls) are indicated by l and CD, respectively (Zanolli et al., 2010)..... 19

LIST OF FIGURES (Continued)

Figure **Page**

2.9 (a) Hysteresis loops of Teflon tape after annealing in pure Ar (black), after storage in a desiccator (red) and after the exposure in air for a long time (blue). (b) Saturation magnetization of Teflon tape subjected to alternative annealing in pure Ar (black full-square) and water steam (blue open square) at 150 °C for 2 h (the violet star represents the as-received tape) (Ma et al., 2012) 20

2.10 First three members of diamondoid series: adamantane, diamantane and triamantane (Meevasana et al., 2009) 22

2.11 sp^1, sp^2, and sp^3 hybridised bonding (Robertson, 2002) 23

3.1 Schematic show our chemical vapor deposition (CVD) system, where the vacuum pump and argon will be used to clean the system 25

3.2 Mechanisms of emission of secondary electrons, backscattered electrons 27

3.3 The interaction of electron beam with specimen and the signal emitted from the sample 27

3.4 Mechanisms of emission of characteristic X-rays from atoms of the sample ... 28

3.5 Types of scattering processes that can occur when light interacts with a molecule 30

3.6 Raman spectra of adamantane powder 30

3.7 Schematic representation of a vibrating sample magnetometer 32

LIST OF FIGURES (Continued)

Figure **Page**

4.1 Color and magnetic responsibility of (a) raw sand and (b) MCS prepared CVD technique using adamantane as a precursor. The SEM micrographs represent the surface morphology with 0.3k magnification of (c) raw sand, (d) MCS and with 30k magnification of (c) raw sand, (d) MCS 34

4.2 Energy dispersive x-ray spectra of MCS, inset reveals the non-magnetic elements signal 35

4.3 (a) M-H hysteresis loop of sand (black), adamantane powder (green) and MCS (red) before subtracting the diamagnetic background. (b) Corrected M-H curves of MCS (red) and boiled-MCS (blue), inset shows the magnified curves near the hysteresis loop center..... 36

4.4 M-H curves of MCS at various temperature between 150 K and 300 K. Inset shows the saturation magnetization increased as measuring at lower temperature..... 38

4.5 Raman spectrum of (black) adamantane powders and MCS (red) shows signals of G-peak, relating for sp^2, D-peak, relating for sp^3 39

4.6 Hysteresis loop of MCS before(red) and after(blue) boiled, inset shows the magnified curves near the hysteresis loop center..... 42

4.7 **(a)** Raman spectrum of MCS (red) and boiled MCS (blue). The curve fitting of the Raman spectrum of (b) MCS and (c) boiled MCS..... 43

4.8 Magnetization curve of MCS (a) before and (b) after steam 2 h 44

LIST OF FIGURES (Continued)

Figure **Page**

4.9 (a) the saturation magnetization (M) of MCS after performing by cyclic of boiling in DI water (blue full circle) and annealing in pure Ar (red full-square) at 150 °C for 2 h, the black full-triangle represents MCS. (b) Raman spectrum of MCS after performing by cyclic of boiling in DI water and annealing in pure Ar at 150 °C for 2 h 44

มหาวิทยาลัยเทคโนโลยีสุรนารี

CHAPTER I

INTRODUCTION

1.1 Motivation

Ferromagnetic materials, which in general consist of metal elements holding the incompletely filled d- or f-orbital such as iron, nickel, and cobalt, have been extensively used in our daily life facilities including electric motors, transformers, and hard disk (Goldman, 1999). Interestingly, ferromagnetism has been reported in various compounds with the absent of magnetic atoms, such as HfO_2, In_2O_3, CeO_2, and Al_2O_3 (Sundaresan et al., 2006 and Coey et al., 2005), and carbon-based materials, such as pyrolytic carbon (Mizogami et al., 1991), graphite (Esquinazi et al., 2003), and Teflon tape (Ma et al., 2012).

Investigations of ferromagnetism in these carbon-based materials have revealed that ferromagnetism in such systems is mainly originated from the intrinsic structural defects, such as vacancies (Zanolli et al., 2010, Lehtinen et al., 2004 and Zhang et al., 2007) and dangling bonds (Ma et al., 2012, Sriplai et al., 2015 and Sangphet et al., 2018). Ferromagnetism in carbon-based materials has received a lot of attention due to their lightweight, flexibility, and low-cost processing (Yu et al., 2012 and Zhang et al., 2014). Up until now, there are researches in the creation and control of unconventional ferromagnetism in carbon-based systems by mechanical methods - e.g. cutting or mechanical stretching (Ma et al., 2012) and high-temperature processing (Sangphet et al., 2018).

In this thesis, we are study ferromagnetism of the carbon films on sand substrate or magnetic carbon sand (MCS) prepared by the chemical vapor deposition (CVD) technique at 1000 °C to create carbon films of adamantane precursor. Furthermore, we aim to study the reduction of magnetization in MCS due to the effect of humidity treatment. We assume that the effect of humidity on MCS's magnetism is caused by water molecules attachment with an unpaired electron or dangling bonds on MCS. We use the boiling process to accelerate the attachment of water molecules and unpaired electron. As sand and adamantane are abundant, cheap, environmentally benign, and harmless to humans, they can be applied in various applications across material engineering and medical sciences for the development of large-scale magnetic shielding and the targeted-drug delivery.

In this chapter, first, we will present our research objectives. After that we will introduce the magnetic properties, including diamagnetism, paramagnetism, ferromagnetism, and we will describe the hysteresis loop characterization Lastly, we will be presented the thesis outline.

1.2 Research objectives

1 To prepare magnetic carbon sand (MCS) by the chemical vapor deposition (CVD) technique using adamantane ($C_{10}H_{16}$) as a precursor.

2 To characterize the morphology and the structure of MCS.

3 To study the magnetic behavior of MCS

4 To study the stabilities of magnetization in MCS through the effect of humidity treatment on its magnetism.

1.3 Magnetic properties

Magnetism refers to physical phenomena describing the ability to attract or repel other materials. The magnetic field can be caused by the motion of electrically charged particles. The magnetic field occurs around the moving electric charges and they disappear when the electric charges stop moving. In the case of permanent magnets, orbits around the nuclei of electrons and electrons spin create the virtual current within the magnet, which is called "Amperian current". This virtual current causes a magnetic field around the magnet. Each material responds differently to the external magnetic field provided. We observed this response by measuring magnetization (M) or magnetic induction (B). Consider at a magnetic placed, if placed at an angle in a magnetic field, a torque acting on a magnet attempts to turn it into parallel the magnetic field, this moment is called "magnetic moment".

In vacuum, the relationship between magnetic induction (B) and magnetic field strength (H) is as in Equation 1.1. Note that μ_0 stands for the vacuum permeability which is $4\pi \times 10^{-7}$ N/A^2

$$B = \mu_0 H \tag{1.1}$$

In matter, when we consider the material placed in applied magnetic field, the magnetic moment will be rearranged into a magnetizing. Therefore, in the case of matter, the relationship between B and H must also be considered by the intensity of magnetization (M). In SI unit, the relationship between B, H and M is as in Equation 1.2

$$B = \mu_0 (H + M) \tag{1.2}$$

when B has units of Weber/m^2 called tesla (T), H and M has unit of A/m. In cgs unit, the relationship between B, H and M is as in Equation 1.3

$$B = H + 4\pi M \tag{1.3}$$

when B has unit of Gauss (G), H has unit of Oersted (Oe) and M has unit of emu/cm^3.

In an experiment, magnetism is often measured in terms of M and then the magnitude of M can tell the magnetic behavior of materials. We can classify magnetic materials according to their response to external magnetic fields. Which can be divided into three main groups which are diamagnetism, paramagnetism, and ferromagnetism.

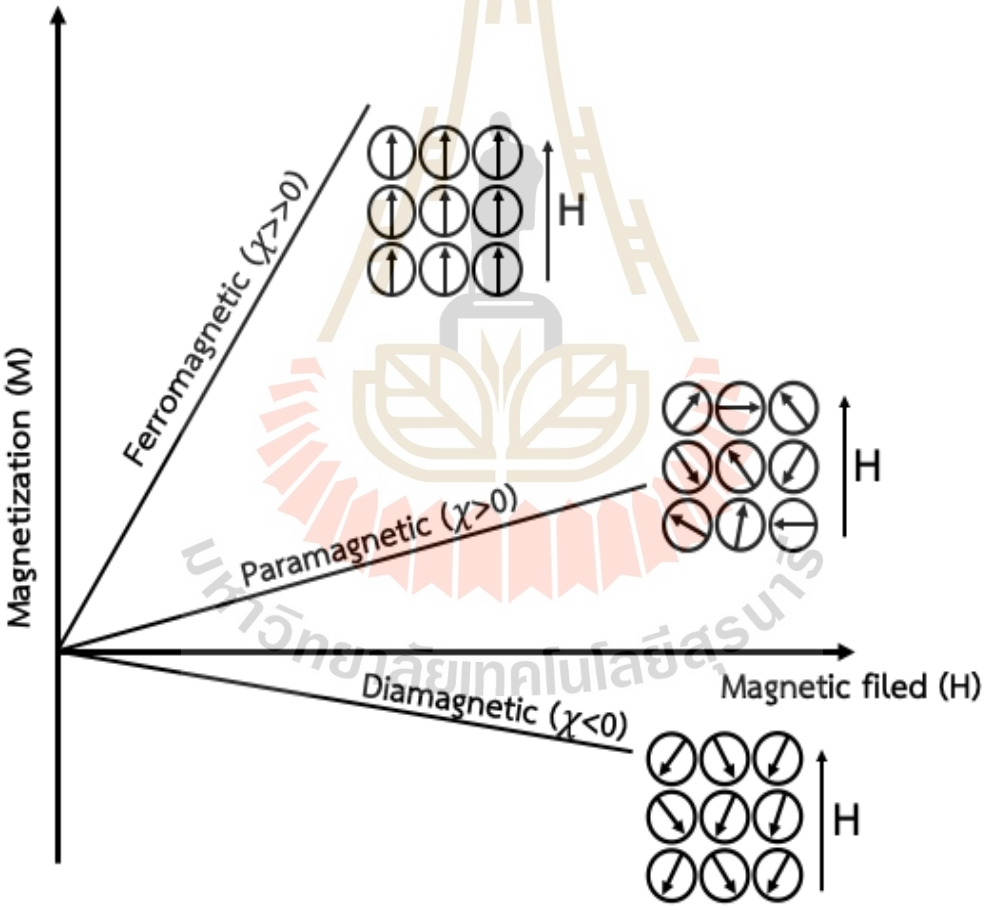

Figure 1.1 Schematic responding of diamagnetic, paramagnetic, and ferromagnetic materials to the presence of a magnetic field H (edit from Pinitsoontorn, 2015).

1.3.1 Diamagnetism

Diamagnetism is a fundamental property of all matter, although it is usually very weak. Figure 1.1 shows that when an external magnetic field is applied to a diamagnetic material, the magnetic moment of the diamagnetic material is arranged in the opposite direction to the external magnetic field. The arrangement of this magnetic moment is induced by a change in the orbital motion of electrons due to an applied magnetic field. In the normal state, for atoms with paired electrons, the magnetic moment due to the orbit of the electrons will cancel out. Diamagnetism occurs when the external magnetic field was applied. This magnetic field causes the change of magnetic moment due to the electron acceleration/retardation in orbit. The diamagnetic property can be observed clearly in materials with all the orbital shells are filled and there are no unpaired electrons. Diamagnetism can be observed clearly in materials with all the orbital shells are filled and there are no unpaired electrons, such as C (diamond), Si, and Ge.

1.3.2 Paramagnetism

Paramagnetism is caused by the atoms or ions in the material have a net magnetic moment due to unpaired electrons in partially filled orbitals. In normal state, no external magnetic field, the magnetic moment is randomly arranged so the net magnetization is zero. When the external magnetic field was applied, a partial alignment of the magnetic moments will in the parallel of the external field, resulting in a net magnetization no zero. In addition, high temperatures result in the arrangement of the magnetic moment returning randomly (at room temperature affects the magnetic moment arrangement).

1.3.3 Ferromagnetism

Ferromagnetic materials exhibit a strong attraction to magnetic fields and are able to retain their magnetic properties after the external field has been removed. Ferromagnetism caused by atoms or ions in the material has unpaired electrons in partially filled orbitals, similar to paramagnetism. The difference is interactions between each magnetic moment in these materials exhibit very strong interactions. In a ferromagnetic material in the unmagnetized state, the magnetic domains are aligned in the same direction and these domains exhibit the net magnetization although in the absence of an external magnetizing field. In addition, if the external magnetic field is reduced, the ferromagnetic material will not decrease linearly, ferromagnetic can retain magnetization even if the external field has been removed. This behavior is called hysteresis. The elements Iron, Nickel, and Cobalt and many of their alloys are common examples of ferromagnetic materials

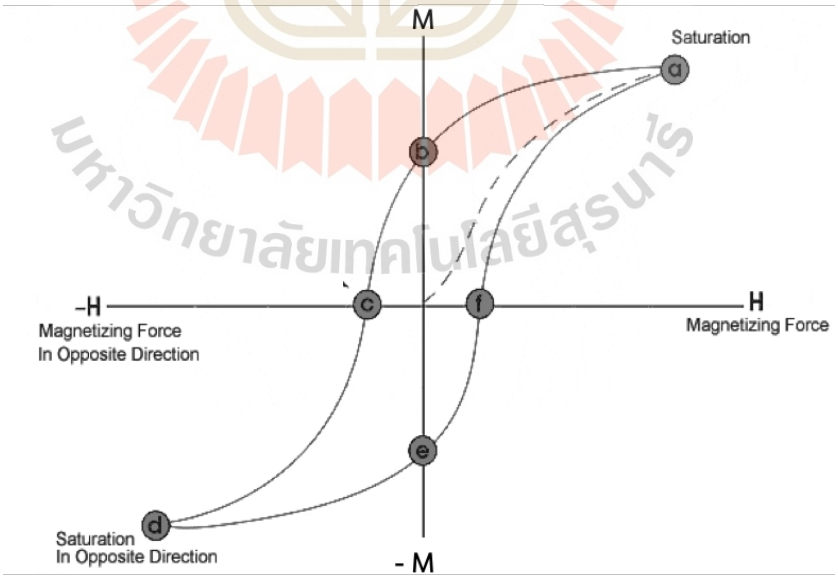

Figure 1.2 Hysteresis loop model of ferromagnetic material.

1.3.4 Hysteresis loop

Hysteresis is a nonlinear response to the external magnetic field of a ferromagnetic material. The hysteresis loop is the curve that shows the relationship between the applied magnetic field (H), and the magnetic flux density (B) or the magnetization (M) of the material magnetized, sometimes this loop is called magnetization curve or M-H curve. Figure 1.2 shown schematic of hysteresis loop of ferromagnetic material. The hysteresis loop is created by measuring the induced flux of ferromagnetic material, magnetized by an applied external field. When magnetizing a magnet, by an applied external field was gradually increased, making the magnetic field stronger, the magnetization will increase due to the alignment of the magnetic domain parallel to the external field. At point (a) is called the saturation magnetization (M_s), the magnetization will never increase due to almost all magnetic domains are aligned in the direction of the applied field. When we decreasing the external field from the saturation point to zero, the magnetization does not return to zero but will decrease to point (b). The remains magnetization of ferromagnetic material even the absence of an applied field is called remanence magnetization (M_r). In order to bring the magnetization value back to zero, a magnetic field in the opposite direction has to be applied, shown in point (c). This magnetic field is called coercivity or coercive force (H_c). By reducing positive the magnetic field gradually, the magnetization of the ferromagnetic will be reduced to point (e). When applied field in a positive direction, the magnetization reduced to zero at point (f), and increase to the saturated point (point a) again. In addition, the characteristics of a hysteresis loop can also indicate soft and hard ferromagnetism. Hard ferromagnetic has H_c or coercivity more than soft ferromagnetic, as shown in Figure 1.3.

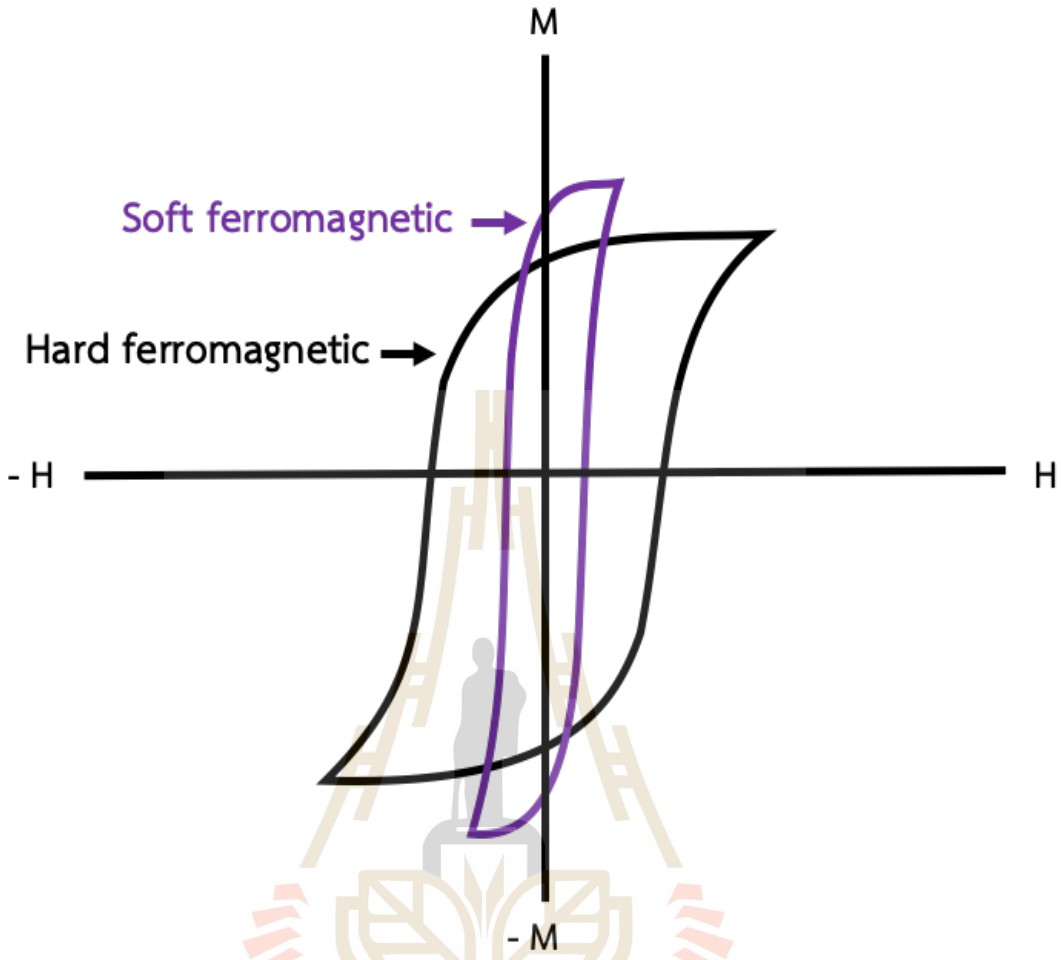

Figure 1.3 Difference between hysteresis characteristics of hard and soft ferromagnetic material.

1.4 Thesis outline

This thesis is divided into five chapters. Chapter I gives a brief overview of the rationale of this research. We introduce the magnetic properties and describe the hysteresis loop characterization which used to study magnetic phenomena. In chapter II, we will present the background studies about ferromagnetism in carbon-based materials and the proposed origins of ferromagnetism. In the last section, we will introduce the background knowledge of diamondoid and adamantane which is a precursor for creating my carbon films on a sand substrate. In chapter III, we will

explain our methodology consisting of the chemical vapor deposition (CVD) technique that is used to prepare carbon films, scanning electron microscopy (SEM), and Raman spectroscopy which used to study the characterization of MCS. Magnetic measurement technique as the vibrating sample magnetometer (VSM) which used to study the magnetic properties of our carbon films and the method to study the effect of humidity treatment on MCS's magnetism is described in the last section of Chapter III. Our results are described in chapter IV. Physical observations, ferromagnetic property, and chemical characterization of our carbon films were reported. After that, the effect of humidity on MCS's magnetism will be presented. In chapter V, we present the conclusion of this work and suggestion for future work.

มหาวิทยาลัยเทคโนโลยีสุรนารี

CHAPTER II

REVIEW OF FERROMAGNETISM IN CARBON-BASED MATERIALS

Normally ferromagnetic materials, which consist of metal elements holding the incompletely filled d- or f-orbital such as Iron, Nickel, and Cobalt and many of their alloys. Interestingly, ferromagnetism has been reported in carbon-based materials, which carbon materials are the materials with only have s- and p-orbital.

Therefore, in this chapter, we will mainly describe the ferromagnetism in carbon materials. In the first section, we will contain literature reviews about the studies of ferromagnetism in carbon-based-materials and the origins of this ferromagnetism. In the second section, we will be giving literature reviews on the effect of environments on ferromagnetism in carbon-based-materials. The final section in this chapter will introduce diamondoid, which used as a precursor material to create our carbon films, and then the knowledge of diamond-like-carbon material will also be described in this section as well.

มหาวิทยาลัยเทคโนโลยีสุรนารี

2.1 Ferromagnetic in carbon-based materials

2.1.1 The studies of ferromagnetism in carbon-based materials

Recently, ferromagnetism in carbon-based systems without magnetic elements have been intensively studied. Investigations of ferromagnetism in these carbon-based materials have revealed that ferromagnetism in such systems is mainly originated from the intrinsic structural defects. There have been reported that those defects can occur

during high-temperature processing, such as the cases of carbon material was prepared by pyrolytic carbon (Mizogami et al., 1991), pyrolysis of polyacrylonitrile (Saito et al., 2011), and graphite (Esquinazi et al., 2003).

Abnormal ferromagnetism in the pyrolytic carbon obtained from adamantane as a raw material was reported by S. Mizogami (Mizogami et al., 1991). The value of the saturation magnetic moments of this pyrolytic carbon was about 0.5 emu/g. They assumed that the origin of ferromagnetism might be attributed to the highly oriented structure of this carbon and a large number of unpaired electrons on the graphite-like. It has been reported that the ferromagnetism in carbon material was prepared by pyrolysis of polyacrylonitrile at 1273 K (Saito et al., 2011), this carbon material exhibited a saturation magnetization of 1.22 emu/g at room temperature. Their results show the different structure of the specimen prepared by pyrolysis exhibited broad peaks in a pattern different from those of polyacrylonitrile precursor, seen in XRD patterns in Figure 2.1. They explained that the observed ferromagnetic behavior of this carbon material is considered to be due to the presence of a graphite-like structure. In 2003, ferromagnetism also has been observed in graphite (Esquinazi et al., 2003). In their research, they have shown evidence that proton irradiation on highly oriented pyrolytic graphite samples triggers ferromagnetism, which the ferromagnetism appears after proton irradiation in graphite and that this is stable at room temperature (see Figure 2.2). Moreover, they believed that the origin for this ferromagnetism in this graphite has been related to the mixture of carbon atoms with sp^2 and sp^3 bonds.

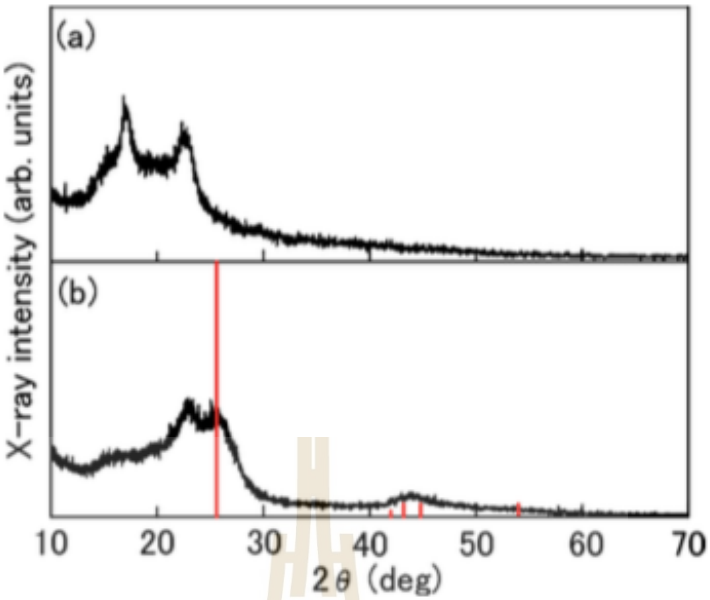

Figure 2.1 XRD patterns of (a) polyacrylonitrile powder and (b) carbon material prepared by pyrolysis of polyacrylonitrile at 1273 K for 1 h. The red straight lines show the usual peak positions of the graphite structure (Saito et al., 2011).

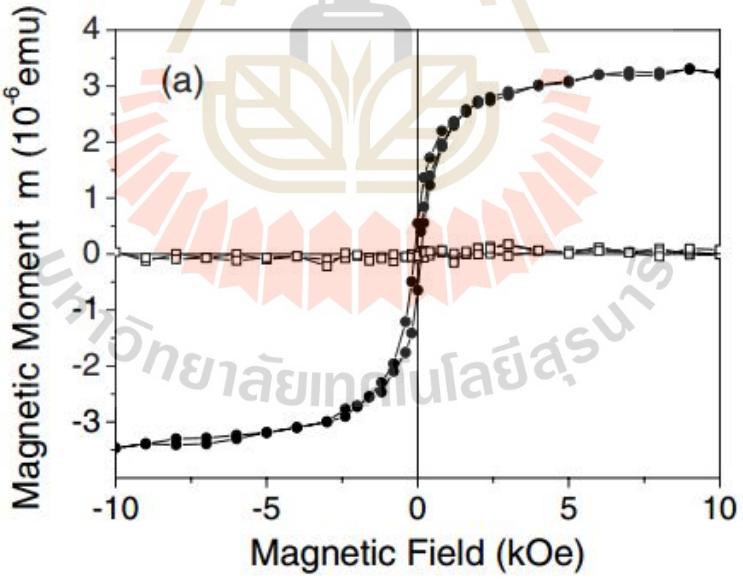

Figure 2.2 Magnetic moment measured at T= 300 K as a function of the magnetic field for highly oriented pyrolytic graphite sample before (□) and after (•) proton irradiation (the background signal was subtracted) (Esquinazi et al., 2003).

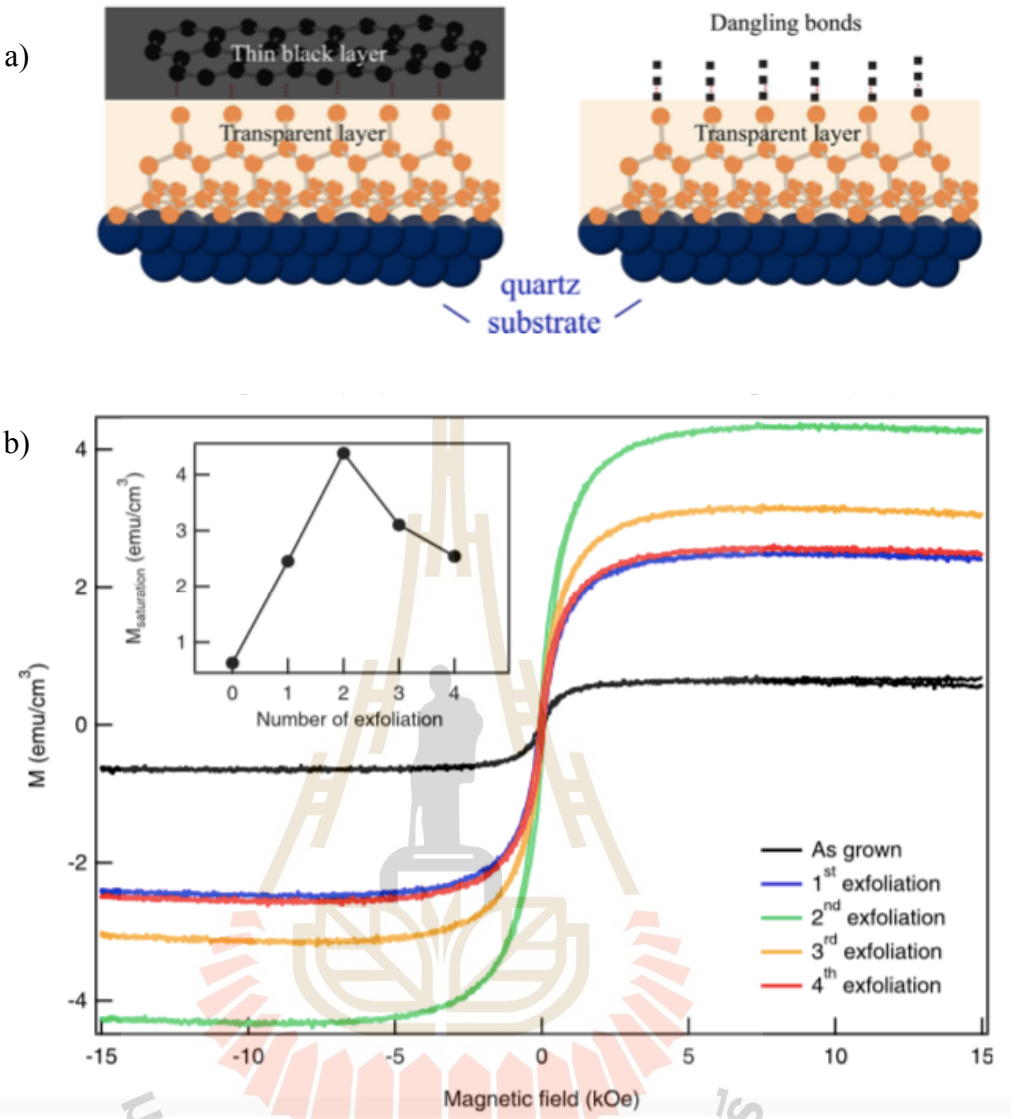

Figure 2.3 (a) Schematic cross-sections of the (left) as-grown and (right) exfoliated regions. After the exfoliation, partially aligned dangling bonds are expected at the surface. (b) Room-temperature magnetization curves, subtracted by diamagnetic background, of as-grown (black), 1st (blue), 2nd (green), 3rd (yellow), and 4th (red) exfoliated CVD-carbon film on a quartz substrate (Sangphet et al., 2018).

Moreover, it has been reported that ferromagnetism can occur in carbon-based systems through very simple methods, such as cutting, mechanical stretching (Ma et al., 2012), and mechanical exfoliation (Sangphet et al., 2018). In our research group has reported ferromagnetism in carbon film (Sangphet et al., 2018) which prepared by chemical vapor deposition or CVD technique. The saturation magnetization of this carbon film is around 0.63 emu/cm^3, which can be further enhanced by mechanically exfoliating the top layers of the films off (show in Figure 2.3(a)); the saturated magnetization can be as large as 4.4emu/cm^3 at room temperature seen in Figure 2.3(b).

2.1.2 Origin of ferromagnetism in carbon-based-materials

The origin of metal-free carbon materials is hard to believe that ferromagnetism can arise from the materials with only have s- and p-orbital. However, the studies of the magnetism in carbon-based materials have also received wide attention, these studies undoubtedly indicate that carbon-based-materials can generate ferromagnetism without magnetic element contaminations. Investigations of ferromagnetism in these carbon-based materials have revealed that ferromagnetism in such systems is mainly originated from the intrinsic structural defects such as dangling bonds and vacancies.

Kim et al. (Kim et al., 2003) proposed that dangling bonds are the cause of ferromagnetism in fullerene. They calculated spin-density of metastable isomer states of C_{60} with dangling bonds may form during cage opening process. A zigzag arrangement of edge atoms in the defective cage creates dangling bonds, which in turn lead to magnetic instabilities in isolated molecules. Figure 2.4 show spin-density isosurfaces for the (a) antiferromagnetic and (b) ferromagnetic spin configurations of the C_{60} cage open.

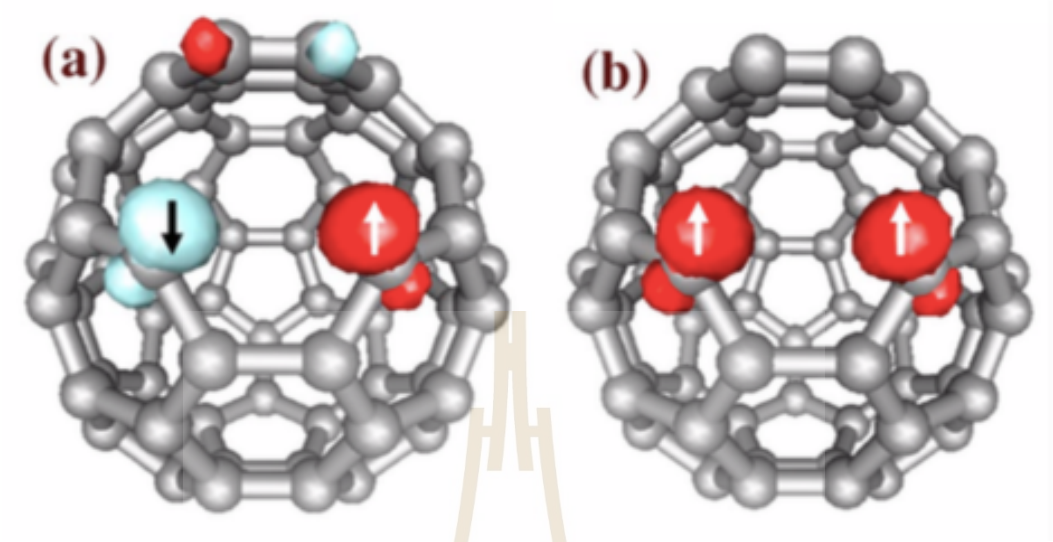

Figure 2.4 Model of (a) antiferromagnetic and (b) ferromagnetic spin configurations of the C60 cage open. (adapted from Kim et al., 2003).

In 2012 (Ma et al., 2012), Ma et al. reported the observation of room temperature ferromagnetism in Teflon tape (polytetrafluoroethylene) which has C chain structure is the backbone by simple mechanical stretching, cutting, or heating. Their experimental results indicate that the ferromagnetism originates from carbon dangling bonds. As proposed in this work, the cutting Teflon tape leading to be formed of carbon dangling bond in the cross-section of the broken tape shows in Figure 2.5(d) and (e). In the case of stretching carbon dangling bonds are largely concentrated on the surface of strain-induced voids shows in Figure 2.5(f) and (g). Each carbon dangling bond carries a magnetic moment of 1 μ_B.

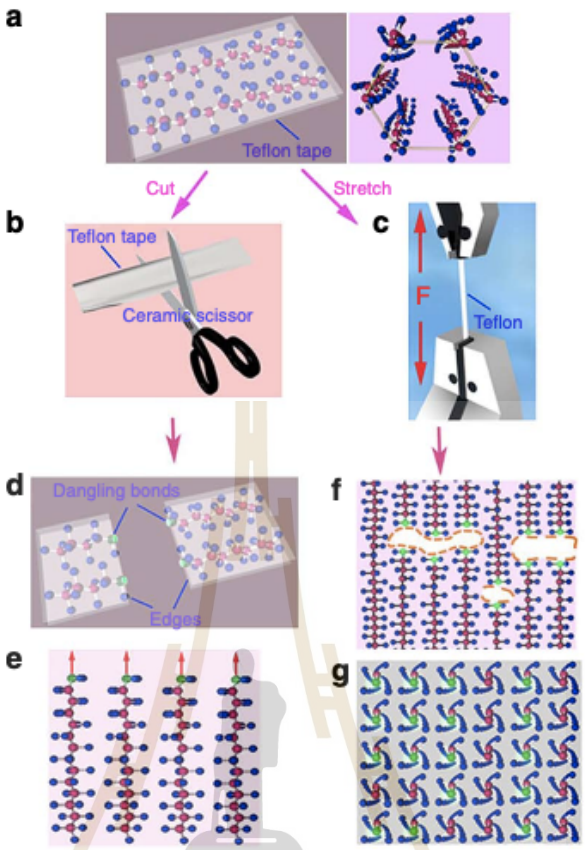

Figure 2.5 Schematic illustration of (a) carbon chain structure in Teflon tape, (b) - (c) cutting and stretching of a Teflon tape, respectively, (d) - (e) dangling bonds created after cutting, and (f) - (g) carbon dangling bonds formed in Teflon by mechanical stretching. (Ma et al., 2012)

In 2003, Andriotis et al. (Andriotis et al., 2003), they reported the calculation of magnetic properties in carbon C_{60} polymers. Their calculated results indicate that onset of magnetism is found to occur in the Rh-C_{60} polymeric phase with defects, which the origin of this magnetism involving an interplay between structural defects and sp^3 hybridization. They calculated accumulated charge at sp^3 bonds and carbon surrounding vacancy. The surrounding vacancy atom and sp^3 bonds in the intermolecular linkage between each pair of C_{60} cages shown in red and green atoms of

Figure 2.6(b), respectively. In the case of C_{60} defect-free, there is an accumulation of excess negative charge in all atoms sp^3 bond. In the case of C_{60} defect-free, there is an accumulation of excess negative charge in all atoms sp^3 bond, whereas, in the case of after created carbon vacancy, they get an excess positive charge. The creation of this carbon vacancy leads to the appearance of excess spin density and net spin magnetic moment associated with each C_{60} molecule.

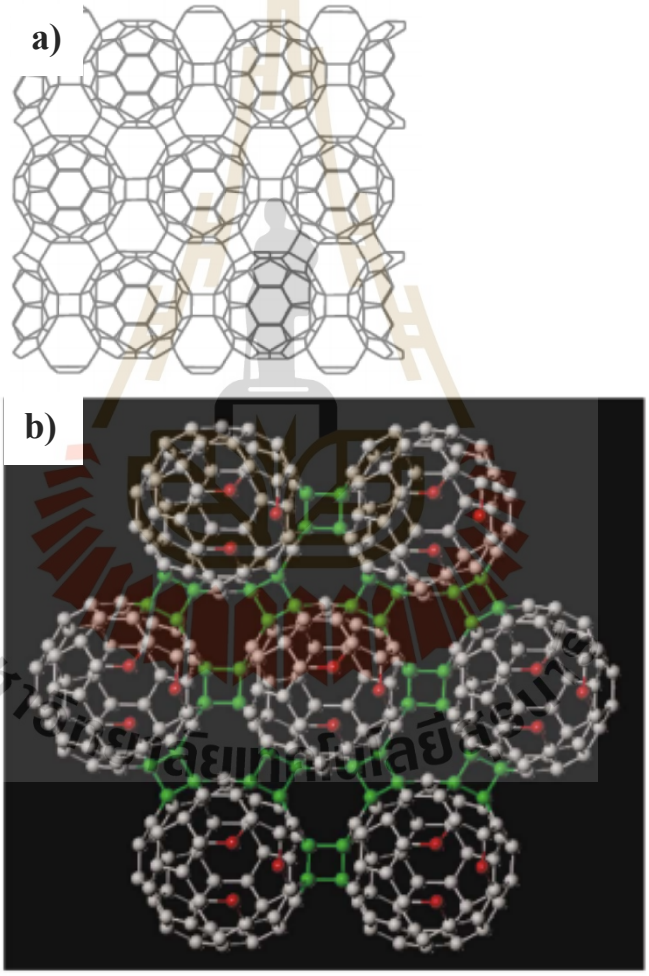

Figure 2.6 Rh-C_{60} polymer without (a) and with (b) one vacancy per C_{60} unit. The atoms surrounding the vacancy are shown in red, while the sp^3 atoms are shown in green (Andriotis et al., 2003).

In the graphite case (Lehtinen et al., 2004), the spin-polarized density functional theory is used to calculate the magnetic properties of irradiation-induced structural defects. When the removal of one carbon atom, each of the three neighboring atoms has one sp^2 dangling bond. Where two of the nearest atoms to the vacancy site saturated by form a weak covalent bond (see in Figure 2.7), resulting in a pentagon-like structure. Their calculations demonstrate that vacancies are magnetic.

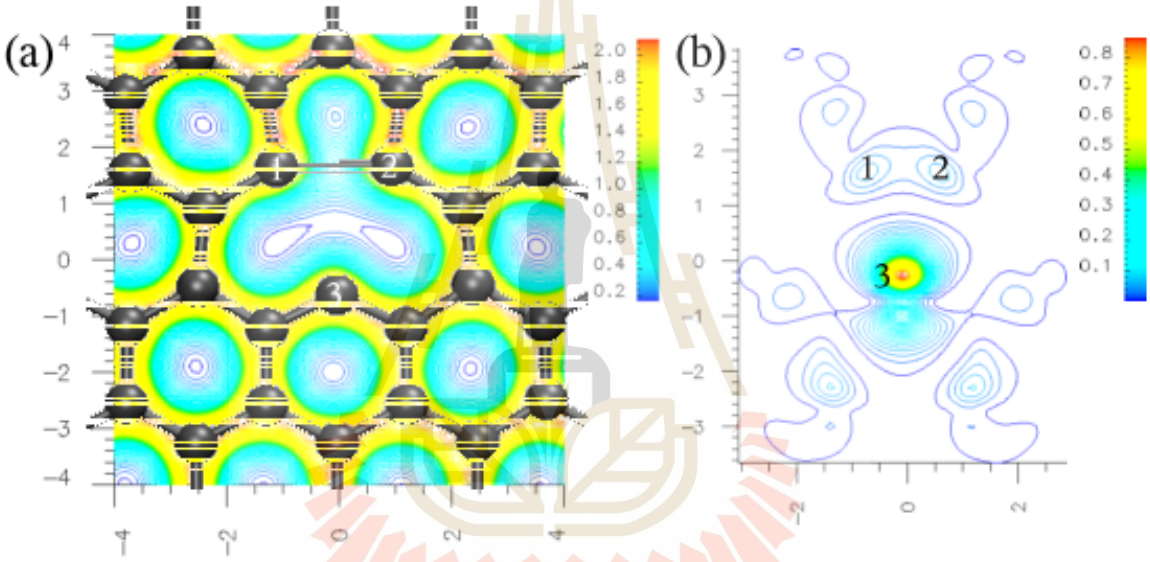

Figure 2.7 (a) Structure, charge density (e/(A^3)˙), and (b) spin density (e/(A^3)˙) of the graphite vacancy. Density plots are slices in the graphene plane (Lehtinen et al., 2004).

Moreover, in case of carbon nanotubes (Zanolli et al., 2010), they studied various geometrical reconstructions of vacancy-defected CNTs by removing one, two, and three carbon atoms from the hexagonal net as shown in Figure 2.8. Figure 2.8(a) demonstrate that removing one carbon atom from a hexagonal net, the three carbon atoms that surround are left with an unsaturated bond. When the system is relaxed, two of the unsaturated carbon atoms will form a weak covalent bond resulting in a

pentagonal rearrangement, and left one carbon atom with an unsaturated bond. In cases of removing two and three carbon atoms the result shows in Figure 2.8(b) and (c).

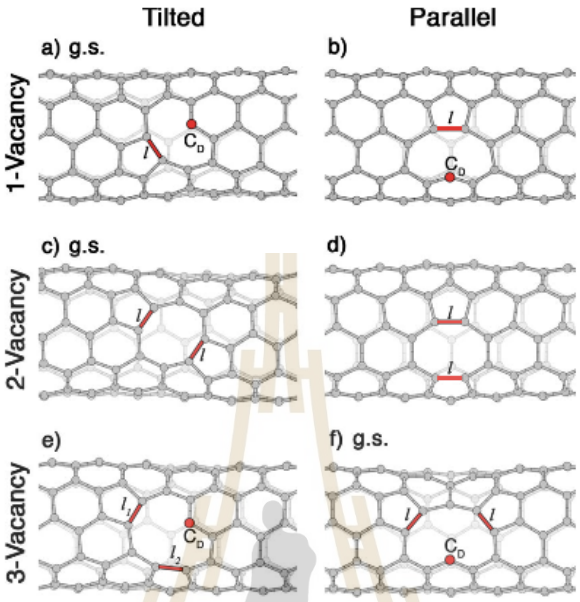

Figure 2. 8 Models atomic structures of a CNT containing a reconstructed monovacancy (a) – (b), divacancy (c) – (d), and trivacancy (e) – (f) in various topological orientations. The newly formed carbon bonds (red sticks) and the dangling carbon atoms (red balls) are indicated by l and CD, respectively (Zanolli et al., 2010).

2.2 Effect of humidity treatment on ferromagnetism in carbon-based materials

In case of Teflon tape, in addition to founding ferromagnetism in Teflon tape, they also study the effects of humidity-filled environments. Ferromagnetism in Teflon tape after annealing in pure Ar is stable under a dry environment after storage in a desiccator for a long time. However, the saturation magnetization is decreased after air exposure for a long time (seen in Figure 2.6(a)). Moreover, they also found that ferromagnetism in Teflon tape does not appear after annealing under water steam. So,

they assume that the decrease in magnetization after a long time of air exposure should be attributed mainly to humidity. It is very interesting, they can be switched “on” and “off” ferromagnetic state in Teflon tape by performing cyclic annealing in Ar and steam, as shown in Figure 2.6(b). They explain that the disappearance of the ferromagnetism in Teflon tape after annealing in steam is caused due to the saturation of C dangling bonds by attachment of water molecules and due to the relatively weak interaction between the C dangling bond and H_2O is thus the reason that ferromagnetism in Teflon tape can be recovered by annealing at an elevated temperature in Ar.

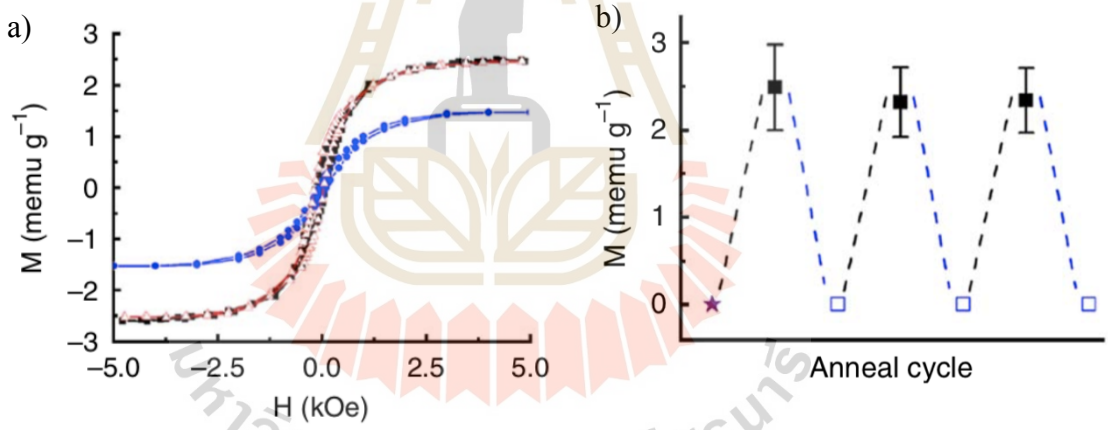

Figure 2.9 (a) Hysteresis loops of Teflon tape after annealing in pure Ar (black), after storage in a desiccator (red) and after the exposure in air for a long time (blue). (b) Saturation magnetization of Teflon tape subjected to alternative annealing in pure Ar (black full-square) and water steam (blue open square) at 150 °C for 2 h (the violet star represents the as-received tape) (Ma et al., 2012).

2.3 Basic knowledge about diamondoid and adamantane

In our research, we study the ferromagnetism in carbon films which using adamantane as a precursor material. Next, we will introduce diamondoid and adamantane.

2.3.1 Diamondoid

Diamondoid molecules are cage-like, saturated nano-hydrocarbons. These molecules are cage compounds, which has a high ratio of C-sp^3:H similar to the nano-diamond and diamond-like-carbon (DLC). Diamondoids have a carbon-carbon framework which is the fundamental repeating unit in the diamond lattice structure. This feature demonstrated that diamondoids are very stable compounds. The general chemical formula of diamondoid is $C_{4n+6}H_{4n+12}$ (where n is the number of diamond cage subunit). Naturally, a diamondoid occurs from petroleum deposits and has been extracted and purified into large pure crystals of polymantane molecules. The first and simplest member of the diamondoids group is called adamantane composing of a single cage. Figure 2.10, illustrates the smaller diamondoid molecules, adamantane ($C_{10}H_{16}$), diamantane ($C_{14}H_{20}$), and triamantane ($C_{18}H_{24}$). Diamondoids have many interesting properties including very low work function (Narasimha et al., 2016) and negative electron affinity (NEA) (Yang et al., 2007).

2.3.2 Adamantane

Adamantane possesses a cage structure with a formula of $C_{10}H_{16}$, the smallest molecule of diamondoids. Adamantane has a high melting point at around 270 °C, which its higher than other hydrocarbons with the same molecular weight. However, adamantane slowly sublimes even at room temperature. One interesting property of adamantane is NEA effect which the vacuum level is below than the conduction band

minimum (Meevasana et al., 2009). These properties are very promising to be used in applications such as photodetectors, electron microscopy, and optical devices (Zhou et al., 2015 and Drummond, 2007).

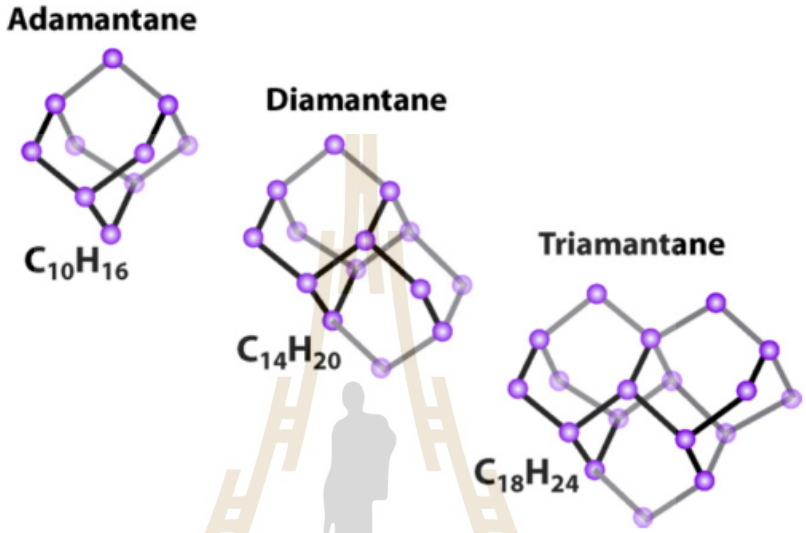

Figure 2.10 First three members of diamondoid series: adamantane, diamantane and triamantane (Meevasana et al., 2009).

2.4 Diamond like carbon

Diamond-like carbon (DLC) is a type of amorphous carbon that shows some common properties of diamonds. DLC exists in many different forms, however, all DLC contains significant amounts of sp^3 hybridized carbon atoms (Robertson, 2002). Normally, carbon has a variety of forms of crystalline and disordered structures due to it can exist in three hybridizations, sp^1, sp^2, and sp^3 (see in Figure 2.11). In the sp^3 configuration, as in diamond, is observed when the mixing character of one 2s-orbital and three 2p-orbitals to create four hybrid orbitals with similar characteristics. This allows four strong q bonds, which demonstrates the strength of the diamond. There are several methods producing DLC, which based on a deposition process such as CVD

technique. DLC film has outstanding properties, such as high mechanical hardness, chemical inertness, and optical transparency, therefore it has been popular in applications.

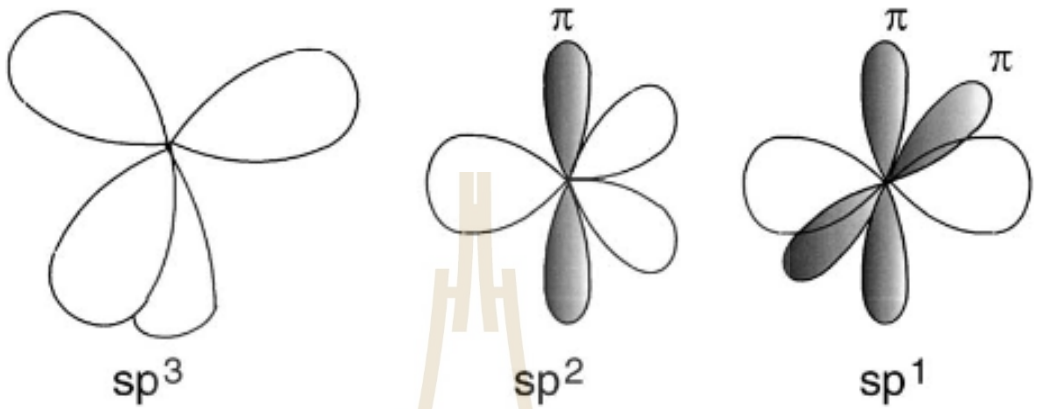

Figure 2.11 sp^1, sp^2, and sp^3 hybridised bonding (Robertson, 2002).

มหาวิทยาลัยเทคโนโลยีสุรนารี

CHAPTER III

METHODS

Our carbon films on sand substrate, which we will so-called magnetic carbon sand (MCS) was prepared by the chemical vapor deposition technique using adamantane as a precursor. Therefore, in this chapter, firstly we will explain the chemical vapor deposition technique. Second, we will introduction scanning electron microscopy (SEM), and Raman spectroscopy which used to study the characterization of MCS. After that, the vibrating sample magnetometer (VSM) which used to study the magnetic properties of our carbon films is described in this chapter. Finally, we will explain the method to study the effect of humidity treatment on MCS's magnetism by boiling process.

3.1 Chemical vapor deposition technique

Chemical vapor deposition (CVD) is a technique that involves depositing a precursor material from a gaseous phase used to create both purity and amorphous films. Before the deposit in CVD-process begins, the coating chamber and substrate are held at a high temperature. This high temperature and the presence of a reducing atmosphere result in the decomposition of precursor molecules which are subsequently deposited onto the surface of the substrate. The precursor gaseous phase generated in an external chamber was transferred to the coating chamber and deposited onto the active surface of the substrate. The purity of the film depends on many parameters,

including the substrate temperature, quality of the atmosphere in the coating chamber, and the active surface of the substrate.

In our CVD system, the carbon films were prepared on sand substrates, the sand is crushed to make similar sizes. The substrate was placed on a holder inside a furnace. The films will be prepared in near-vacuum with the pressure around 10^{-5} torrs. For deposition as a film, we heated the substrate from room temperature until around 1,050 °C, and then the adamantane precursor gaseous phase generated in an external chamber was transferred to a furnace chamber.

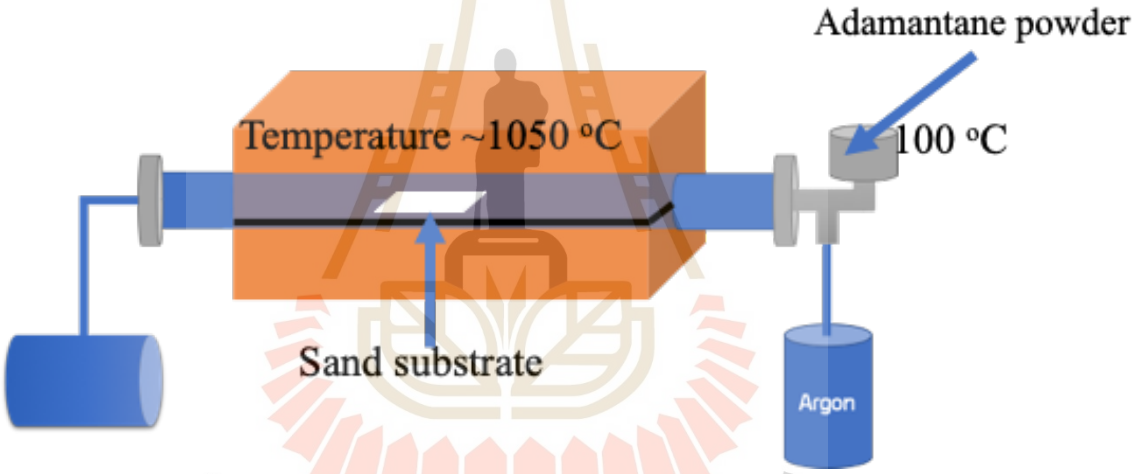

Figure 3.1 Schematic show our chemical vapor deposition (CVD) system, where the vacuum pump and argon will be used to clean the system.

3.2 Scanning electron microscopy (SEM)

Scanning electron microscopy (SEM) is an important technique of electron microscopy that is used to generate a detailed visual image of materials with high-quality and spatial resolution. The SEM instrument is based on the principle that accelerated electrons carry of kinetic energy, and provide electron signals produced when these electrons interact with the atom of the specimen. These electron-specimen

interactions will emit a variety of signals due to electric charge field interaction of incoming electrons with specimen nucleus and electrons, including secondary electrons (SEs), backscattered electrons (BSE), photons (characteristic X-rays that are used for elemental analysis and continuum X-rays), visible light (cathodoluminescence-CL), and heat. The two commonly used electrons for image creation are the secondary electrons and backscattered electrons. Secondary electrons originate from the atoms of the sample, they are a result of inelastic interactions between the electron beam and the specimen. The location of secondary electron productions that are very close to the sample surface, so, secondary electrons are an important signal for showing morphology and topography on samples. Backscattered electrons originate from the primary electron beam that is reflected back after elastic interactions between the electron beam and the specimen. Secondary and backscattered electrons escape from different depths of the sample, backscattered electrons escape from a depth of several times greater than the depth of secondary electrons (shown in Figure 3.3), and therefore their energy remains different. Backscattered electrons images contain information for illustrating the contrast of different atom in the sample, the higher the atomic number, the brighter the material appears in the image. X-ray generation is produced by inelastic scattering of the primary electrons with inner shell electrons of atoms in the sample, this characteristic is used for elemental analysis.

In this work, scanning electron microscopy (SEM, ZEISS Auriga) was used to characterize the morphology of the MCS, organized by The Center for Scientific and Technological Equipment (CSTE), Suranaree University of Technology.

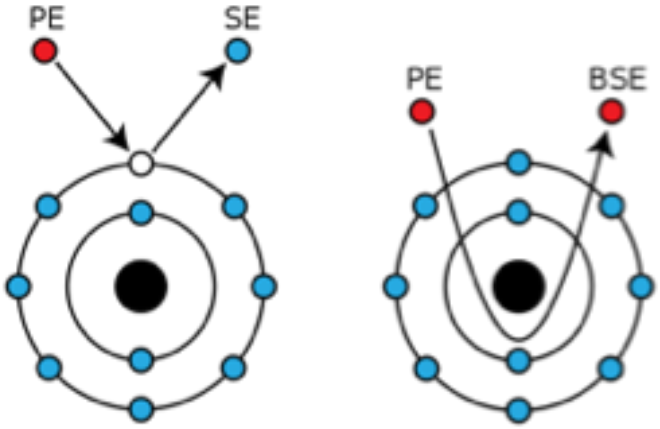

Figure 3.2 Mechanisms of emission of secondary electrons, backscattered electrons.

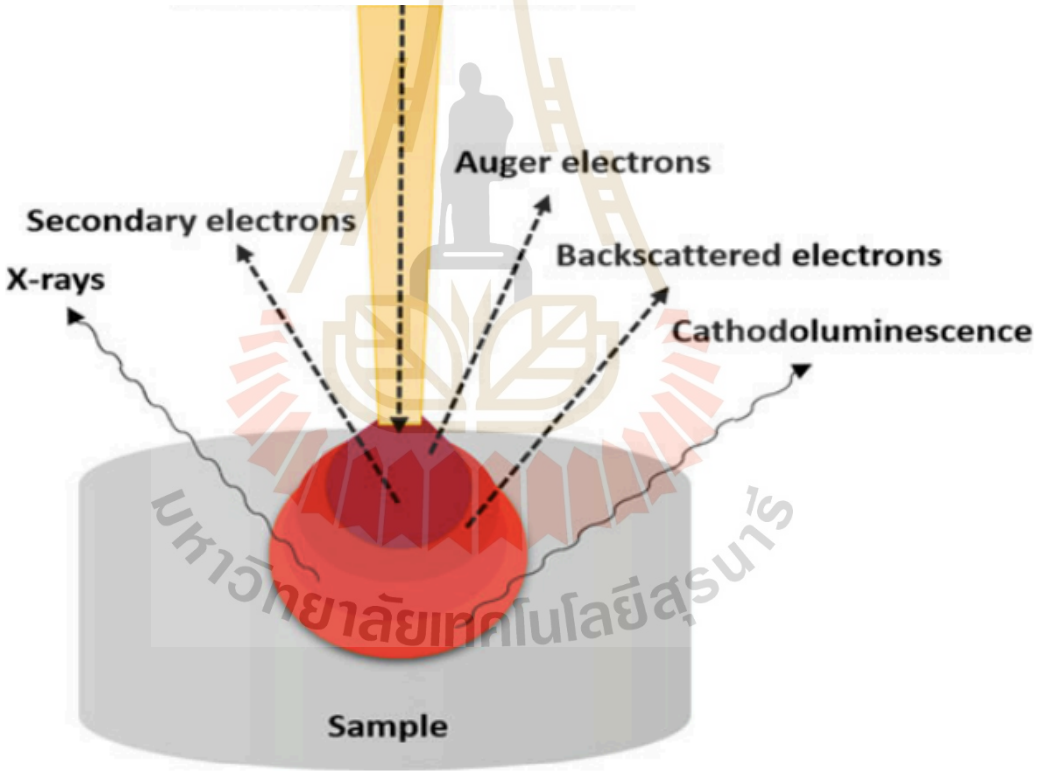

Figure 3.3 The interaction of an electron beam with specimen and the signal emitted from the sample.

3.3 Energy dispersive X-ray spectroscopy (EDS)

Energy-dispersive X-ray spectroscopy (also known as EDS, EDX, or EDXA) is a standard technique that enables the user to identify and quantifying elemental compositions in a specimen. As mentioned in section 3.2, the electron beam excites the atoms on the sample surface, electrons are ejected from the atoms comprising the sample surface. The electron vacancies are filled by electrons from a higher state, and then those atoms emitting specific wavelengths of X-rays that are characteristic of the atomic structure of the elements (see in Figure 3.4). These characteristics X-ray emitted of different wavelengths or different energy can be detected by energy dispersive spectrometer. When an incident x-ray incident with the detector, it creates a charge pulse that is proportional to the energy of the x-ray. The charge pulse is converted to a voltage pulse, which remains proportional to the x-ray energy. The limitations of EDS is cannot measure the light elements (such as H and He) and its detection limits are about 1000 ppm by weight.

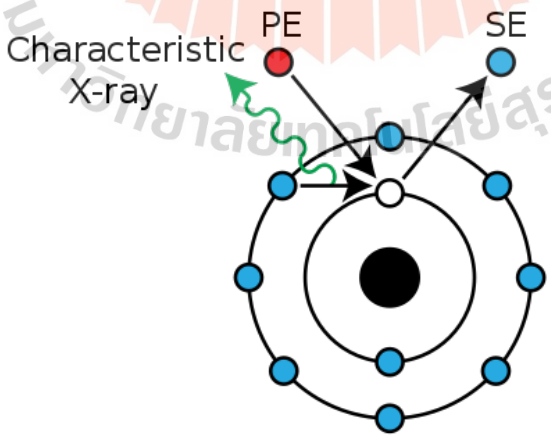

Figure 3.4 Mechanisms of emission of characteristic X-rays from atoms of the sample.

3.4 Raman spectroscopy

Raman Spectroscopy is a nondestructive and requires little sample preparation, that provides detailed information about chemical structure, chemical bonding, and intramolecular bonds. This technique is based on inelastic light scattering with the chemical bonds within a material and observed vibrational modes and frequency modes. In general, Raman spectroscopy uses a monochromatic light source. When a high-intensity light is irradiated on molecules of the specimen, a molecule scatters incident light. General, the scattered light is both elastic and inelastic (shown in Figure 3.5). Most of the scattered light has the same wavelength as the light source, this is elastic scattering light and it's called Rayleigh Scatter. However, a small amount of light is scattered has different wavelengths from the incident light, due to the interaction between the oscillation of light and molecular vibration. This is inelastic scattering light and it's called Raman Scatter. Due to this change in wavelength is specific to molecular vibration and phonon, therefore use this information to analyze the composition of the material information by analyzing the spectrum of Raman scattered light. Raman spectrum showing the intensity and wavelength position of the Raman scattered light. Each peak corresponds to a specific molecular bond vibration, including individual bonds. Figure 3.6 shows an example of the Raman spectra of adamantane.

In this work, to obtain information on the structure in our MCS were characterized by Dispersive Raman spectroscopy (Bruker, Senterra II), organized by Synchrotron Light Research Institute (SLRI) using a green laser of 532 nm at a power of 12.5 mW.

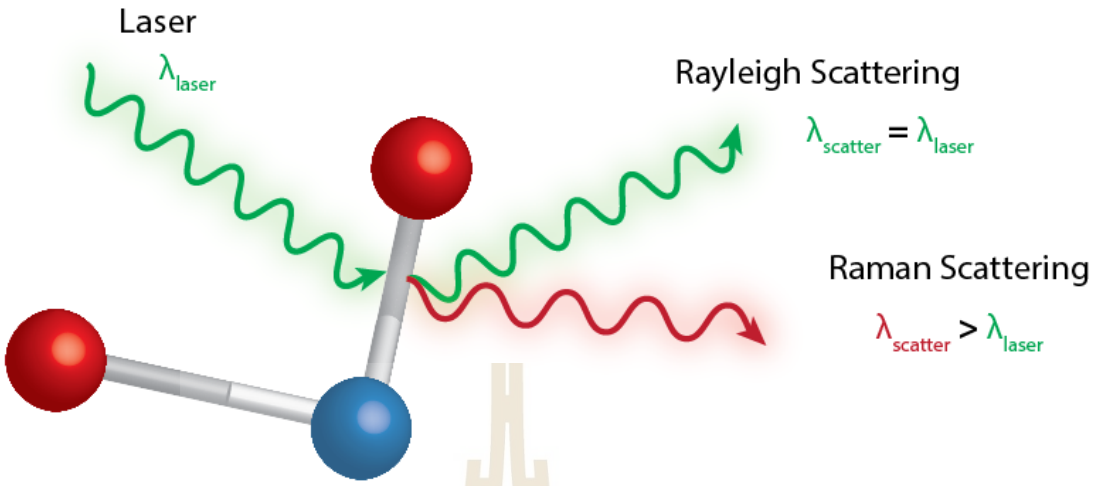

Figure 3.5 Types of scattering processes that can occur when light interacts with a molecule.

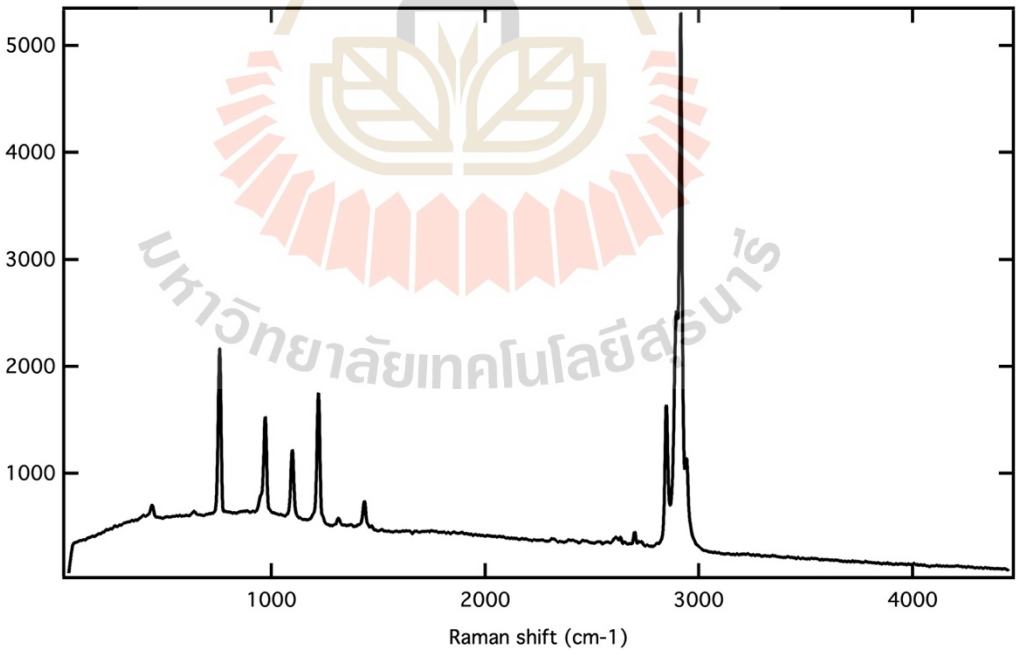

Figure 3.6 Raman spectra of adamantane powder.

มหาวิทยาลัยเทคโนโลยีสุรนารี

3.5 The vibrating sample magnetometer

The vibrating sample magnetometer (VSM) is one of the instruments used to measure the magnetic moment of a sample with very high precision. A vibrating sample magnetometer based on Faraday's Law of Induction, which describes that a changing magnetic field or magnetic flux (Φ) will generate an electric field, as shown in equation 3.1. This electric field can tell us information about the changing magnetic field.

$$\varepsilon = -\frac{d\Phi}{dt} \tag{3.1}$$

In the VSM measurement setup, the sample which is fixed to the sample rod is placing in a constant and uniform external magnetic field which induces a magnetization in the sample by aligning the magnetic domains. The change in magnetic flux will originate when the sample is then vertically vibrated in a uniform external magnetic field. This magnetic flux is changing as a function of time and can be sensed by a set of pick-up coils. A schematic for VSM is shown in Figure 3.7. The uniform external magnetic field varies over a given range, and a plot of magnetization (M) versus magnetic field strength (H) is generated, this plot called the hysteresis loop.

In this work, we used VSM to study the magnetic property of MCS, the VSM (the Quantum Design VersaLab Instrument) organized by Khon Kaen University, operated at the applied magnetic field between -15 and 15 kOe.

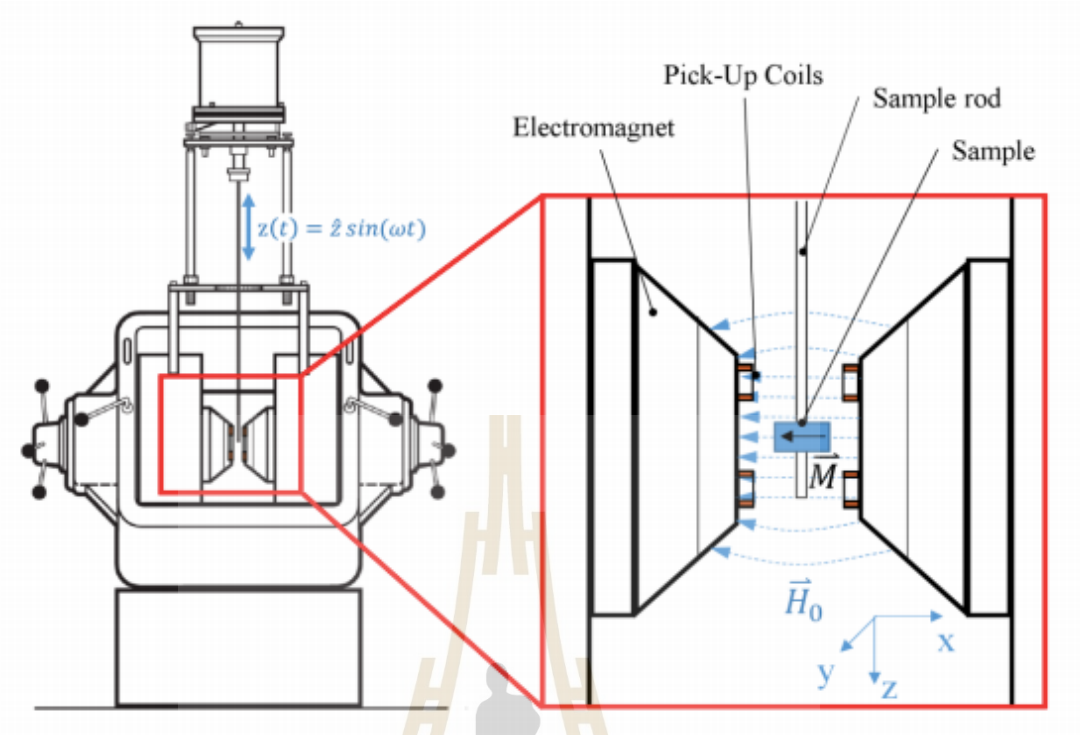

Figure 3.7 Schematic representation of a vibrating sample magnetometer.

3.6 Study effect of humidity treatment on MCS's magnetism

To study the effect of humidity treatment on the ferromagnetism of MCS. We use the boiling process to accelerate the attachment of water molecules and carbon films on MSC. The MCS will be boiled in DI water at 150 °C until the DI water evaporates completely. We will measure the magnetism of the MCS before and after the boiling process by VSM.

CHAPTER IV

RESULTS AND DISCUSSION

The ferromagnetism behavior can be observed in the carbon film on the sand substrate, which we called MCS, prepared by CVD technique which using adamantane as a precursor. The physical properties of MCS were studied by scanning electron microscopy, we will be shown in section 4.1. The elemental analysis of the MCS was performed by using energy dispersive x-ray spectroscopy equipped on SEM, which will also be described in this section. Section 4.2 demonstrates ferromagnetism in MCS which measured by the vibrating sample magnetometer. Ferromagnetism in MCS could be decreased after the specimen attachment with humidity, will also be presented in this section. In order to study the ferromagnetism occurring in our sample, the Raman spectrum is used to characterize the changed structure of adamantane before and after the CVD process, which described in section 4.3.

4.1 Characterization of the MCS morphology

4.1.1 Physical characteristics of MCS

As mentioned in Chapter III, regarding the MCS preparation, we use adamantane powder to prepared carbon film on the sand substrate by CVD-technique. Figures 4.1(a) and 4.1(b) show the color and magnetism behavior of a raw sand and MCS. It is clearly seen that its color change from white to black as well as the switching of magnetism from non-responsive to attractive with a permanent magnet. Non-magnetic raw sand grains after coated with carbon films by CVD technique could stick

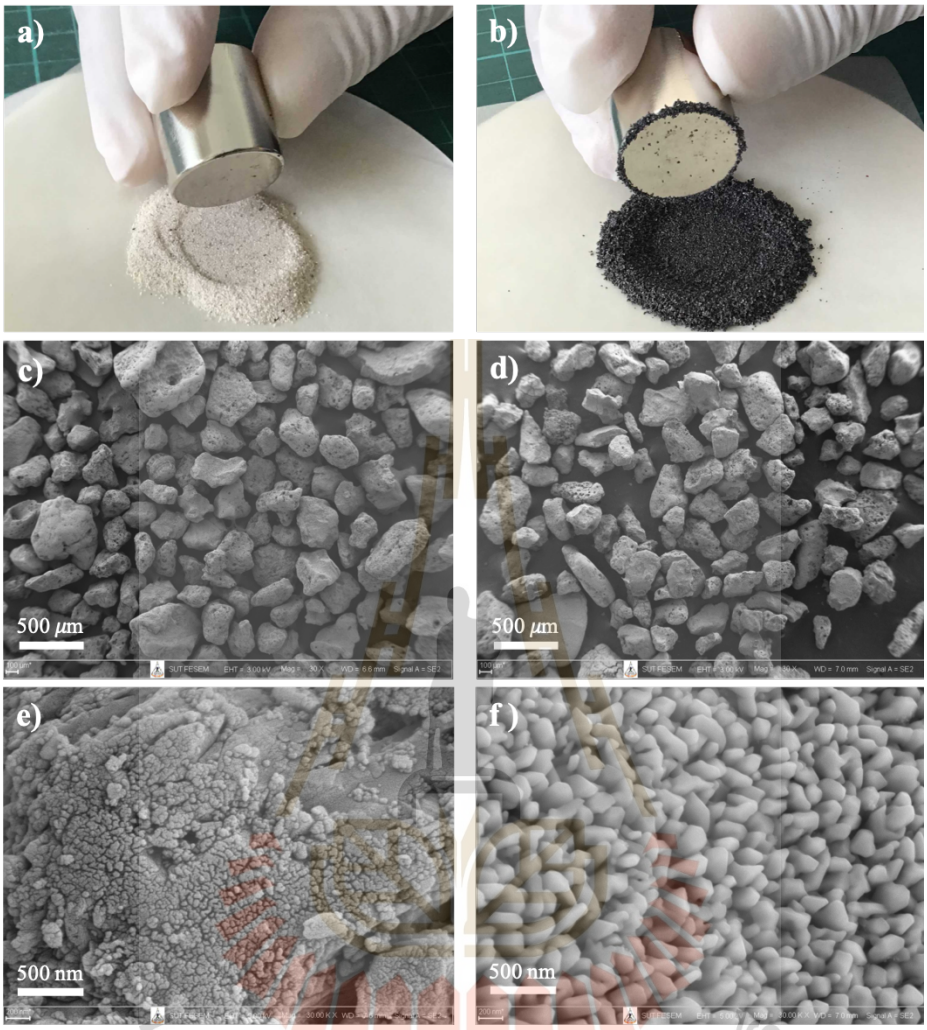

Figure 4.1 Color and magnetic responsibility of (a) raw sand and (b) MCS prepared CVD technique using adamantane as a precursor. The SEM micrographs represent the surface morphology with 0.3k magnification of (c) raw sand, (d) MCS and with 30k magnification of (c) raw sand, (d) MCS.

to around the edges of a strong permanent magnet. This response to permanent magnets demonstrated the occurrence of weak ferromagnetic properties in these grains sand coated with carbon film. Figures 4.1(c), (e) and Figures 4.1(d), (f) show the SEM images of raw sand and MCS whose morphologies change from a very rough surface to the spreading of the irregular shaped particles over the whole surface, and the size of

each irregular shaped particles is approximately 200 nm. This solid difference of their surface morphologies suggests the formation of carbon particles on sand which may play an important role in the observed ferromagnetism in MCS.

4.1.2 Energy dispersive x-ray spectroscopy of MCS

In order to verify that the magnetic saturation values that appear are not from magnetic metals (such as Fe, Ni, and Co) which are enough to explain our signal. We used EDS to observe the elements that are elements of MCS, which we found four main elements: C, O, Ca and Si, at various positions of the sample as shown in Figure 4.2). We have observed no trace of magnetic elements (signals of Fe, Ni, and Co are located at 6.398 eV, 6.924 eV, and 7.471 eV respectively), within experimental error.

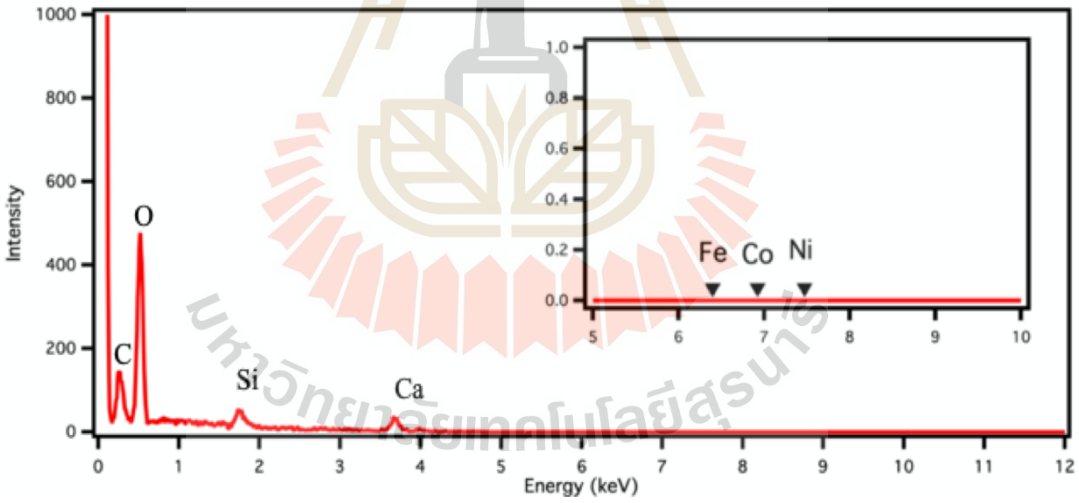

Figure 4.2 Energy dispersive x-ray spectra of MCS, inset reveals the non-magnetic elements signal.

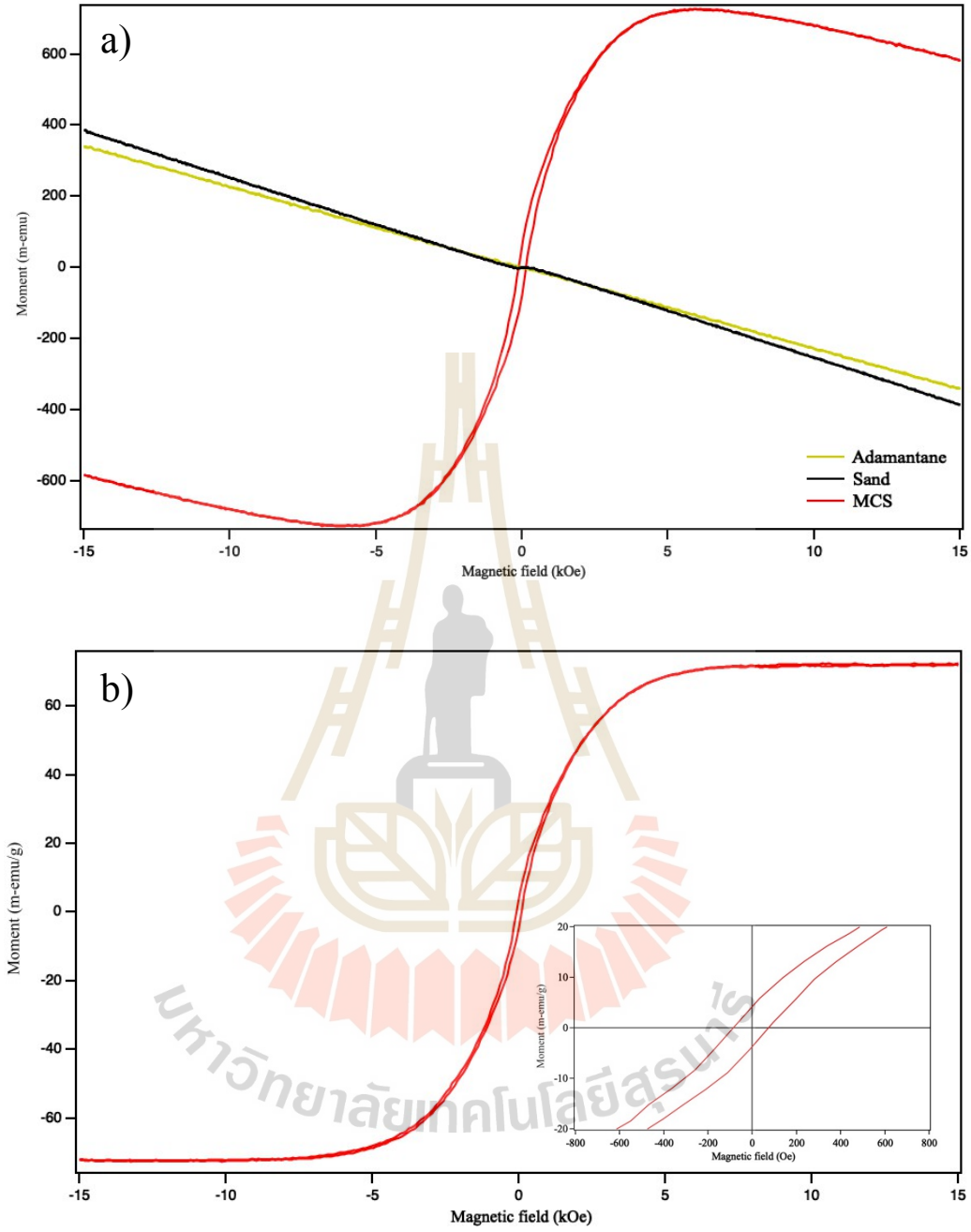

Figure 4.3 (a) M-H hysteresis loop of sand (black), adamantane powder (green) and MCS (red) before subtracting the diamagnetic background. (b) Corrected M-H curves of MCS (red), inset shows the magnified curves near the hysteresis loop center.

4.2 The magnetic property of MCS

Figure 4.3(a) shows the M-H curves of raw sand (black line), adamantane (green line), and MCS (red line) measured using VSM. We applied the external magnetic field in the range between -15000 and 15,000 Oe at room temperature. It is seen that the adamantane powder and raw sand present diamagnetic behavior while the MCS exhibits the mixed between ferromagnetic and diamagnetic features. To analyze the saturation magnetization, the magnetic signal of MCS has been corrected by subtracting its curves by the diamagnetic signal. The corrected MCS signal is shown by the red curve in Figure 4.3(b). The saturation magnetization (M_{total}) calculated using the total mass (sand and carbon mass) after subtraction the diamagnetic signal was observed with to be around 72 m-emu/g. We then calculate the lower-bound value of the saturation magnetization of the only carbon film (excluding the mass of sand) by knowing that the mass ratio between adamantane precursor and sand particles (0.15 g/ 2 g = 0.075) and hence if all the adamantane precursor remains on sand particles after the CVD process, the lower-bound value is then equal to 72 m-emu/g divided by this ratio 0.075 or approximately ~1 emu/g. This value is higher than the previous magnetic carbon-films (Sangphet et al., 2018, Saito et al., 2011). However, the adamantane precursor is not completely coated on the sand substrate, since there is still a carbon film coated in the coating tube chamber. In addition, inset Figure 4.3 shows the magnified curves near the hysteresis loop center. This indicates that the magnetization value of MCS back to zero or coercivity point (H_c) when a magnetic field in the opposite direction has to be applied is around 100 Oe.

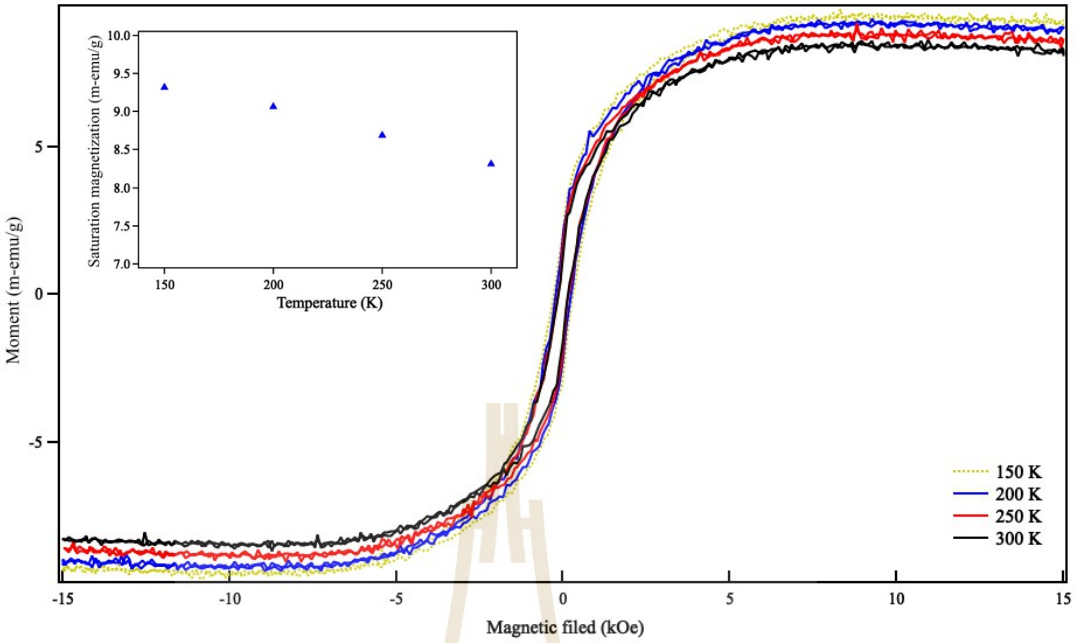

Figure 4.4 M-H curves of MCS at various temperature between 150 K and 300 K. Inset shows the saturation magnetization increased as measuring at lower temperature.

Moreover, we also study the relationship between temperature and the saturation magnetization of MCS. The saturation magnetization of this specimen increases as temperature decrease as indicated by the hysteresis loop of our MCS at various temperatures between 150 K and 300 K as shown in Figure 4.4. Inset Figure 4.4 shows the saturation magnetizations of this MCS at various temperatures. Note that the specimen, used in this study of temperature dependence, is prepared from uncrushed sand, therefore, the size of MCS prepared from sand grains is larger than MCS prepared from crushed sand (the ratio of carbon to total mass is less).

4.3 Raman spectrum of MCS

As proposed in other investigations of ferromagnetism in carbon-based materials, it has been suggested that the ferromagnetism in such systems are originated from the intrinsic structural defects. For example, ferromagnetic behavior can be

observed in such carbons prepared by either pyrolysis or the CVD techniques (Sangphet et al., 2018, Saito et al., 2011) at around 1,000 °C which suggests the emergence of unpaired electrons due to the structural defects in the graphite-like structure. As seen in our Raman spectrum (Figure 4.5), there is a clear difference between the adamantane feature and our MCS. The Raman peak positions of MCS reveal the D peak at around 1,349 cm^{-1}, corresponding to disorder of carbon bonding, the G peak at around 1,591 cm^{-1} corresponding to sp^2 bonding or graphite peak. This feature indicates that the adamantane becomes the graphite-like structure after the CVD process. In addition, structural defects may occur during the CVD process with temperatures up to 1050 °C. Here, it could be concluded that the ferromagnetic behavior observed in our MCS is attributed to the structural defects of the formation of graphitic carbon film on the sand.

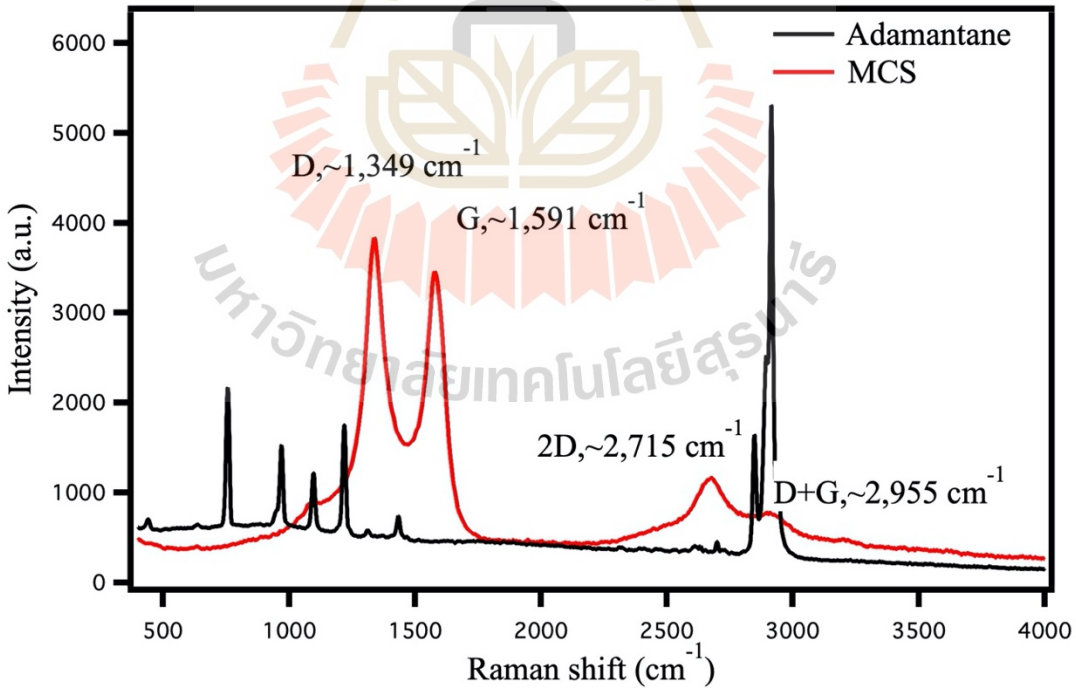

Figure 4.5 Raman spectrum of (black) adamantane powders and MCS (red) shows signals of G-peak, relating for sp^2, D-peak, relating for sp^3.

4.4 Effect of humidity treatment on MCS's magnetism

Moreover, we also study the effect of humidity treatment on the ferromagnetism of MCS by boiling our sample in DI water to accelerate the attachment of water molecules and carbon films. The blue curve in Figure 4.6 shows the M-H curve of the boiled-MCS whose saturation magnetization was observed to be decreased from 72 m-emu/g to 53 m-emu/g. By focusing on the mechanism during the humidity treatment, there are at least two possible scenarios occurring upon boiling which are the adsorption of water molecules and carbon peeling. In the first case, the decrease of saturation magnetization in boiled-MCS might be achieved if water molecules are attached on the surfaces of MCS similar in the case of water-annealed Teflon tape (Ma et al., 2012). The decrease of magnetization could be described by the saturated of unpaired electrons or dangling bonds where those defects are eliminated when attached to the water. To support this assumption, we have measured the Raman spectrum of MCS before and after boiling in DI water. Figure 4.7(a) shows the Raman spectra of MCS (red) and boiled-MCS (blue). Raman spectra of boiled-MCS reveal the peak at around 3651 cm^{-1}, which corresponding to a peak of water. Note that S.H. Park has reported that the Raman shift of water vapor is 3657 cm^{-1} (S.H. Park et al., 2010). This feature in the Raman spectrum demonstrates that water molecules are attached to MCS after boiled in DI water. In addition, the ratio of G and D peak area (A_G/A_D) decreased after boiling. The average ratio of G and D peak intensities before and after boiling was 0.95 and 0.79, respectively. Figure 4.7(b) and (c) shows the curve fitting of the Raman spectrum of MCS and boiled MCS, respectively. Moreover, then steaming also causes a similar effect on MCS's magnetism as boiling. We have steamed our samples which have reduced the saturation magnetization of MCS. Figure 4.8 shows the magnetization

curves of MCS before and after steam. We note that the effect of carbon peeling may not play a significant role in the decrease of magnetization because 1) there is no significant change in the total mass of our MCS after boiling and 2) if the surface is peeled, they may result in more carbon dangling bonds which can increase the magnetization instead (Sangphet et al., 2018).

To further understand the effects of humidity on the magnetic property of MCS, the cyclic of boiling in DI water and annealing in Ar at 150 °C for 2 h was performed. Using MCS with the average saturation magnetization of 74 m-emu/g, and then the saturation magnetization of MCS decreases after boiled in DI water. Moreover, we found that the saturation magnetization can be recovered by annealing in Ar gas at 150 °C even though it isn't fully recovered. The saturation magnetization of MCS can be decreased and recovered by performing cyclic between boiling in DI water and annealing in Ar gas, as shown in Figure 4.9(a). The presence of water molecules in MCS was examined using Raman spectroscopy. A peak at Raman shift of 3,651 cm^{-1}, assigned to adsorbed water molecules, was found in the MCS after boiled (shown in Figure 4.9(b). After annealing in Ar, the peak intensity decreased, however, it increased again with a similar intensity after boiled and decreased again after annealing in Ar gas. In addition, the Raman spectrum also shows the change of A_G/A_D after performing each step of cyclic between boiling in DI water and annealing in Ar. This ratio decreased after the MCS was boiled in DI water and increased after the MCS was annealed in Ar. However, the change of this ratio in the second time of MCS after performing cyclic between boiling and annealing was less than that of the first time.

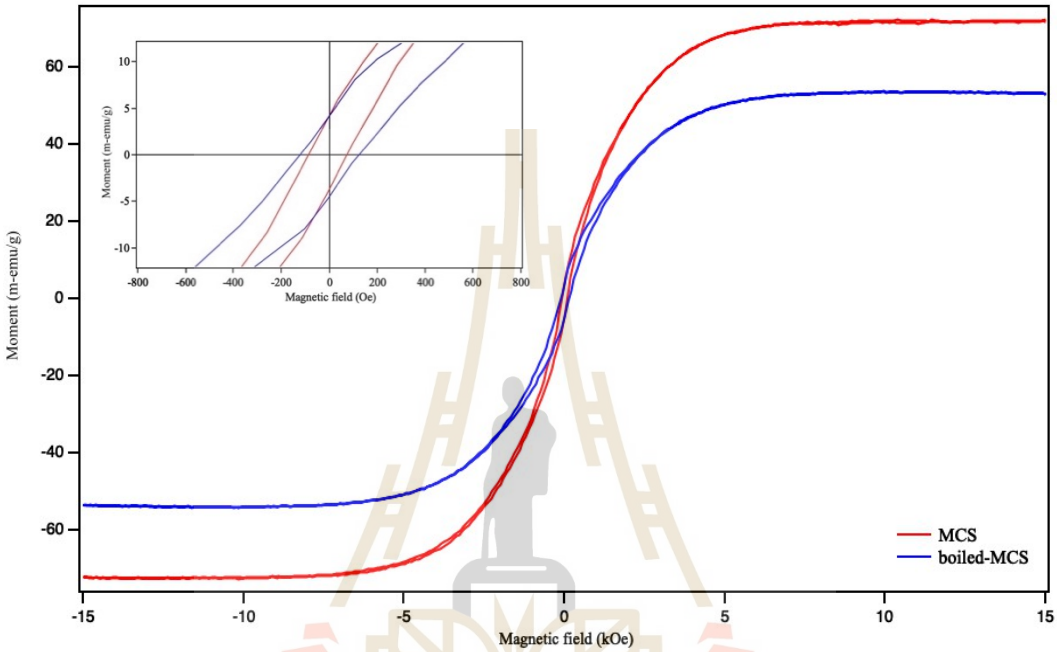

Figure 4.6 Hysteresis loop of MCS before(red) and after(blue) boiled, inset shows the magnified curves near the hysteresis loop center.

มหาวิทยาลัยเทคโนโลยีสุรนารี

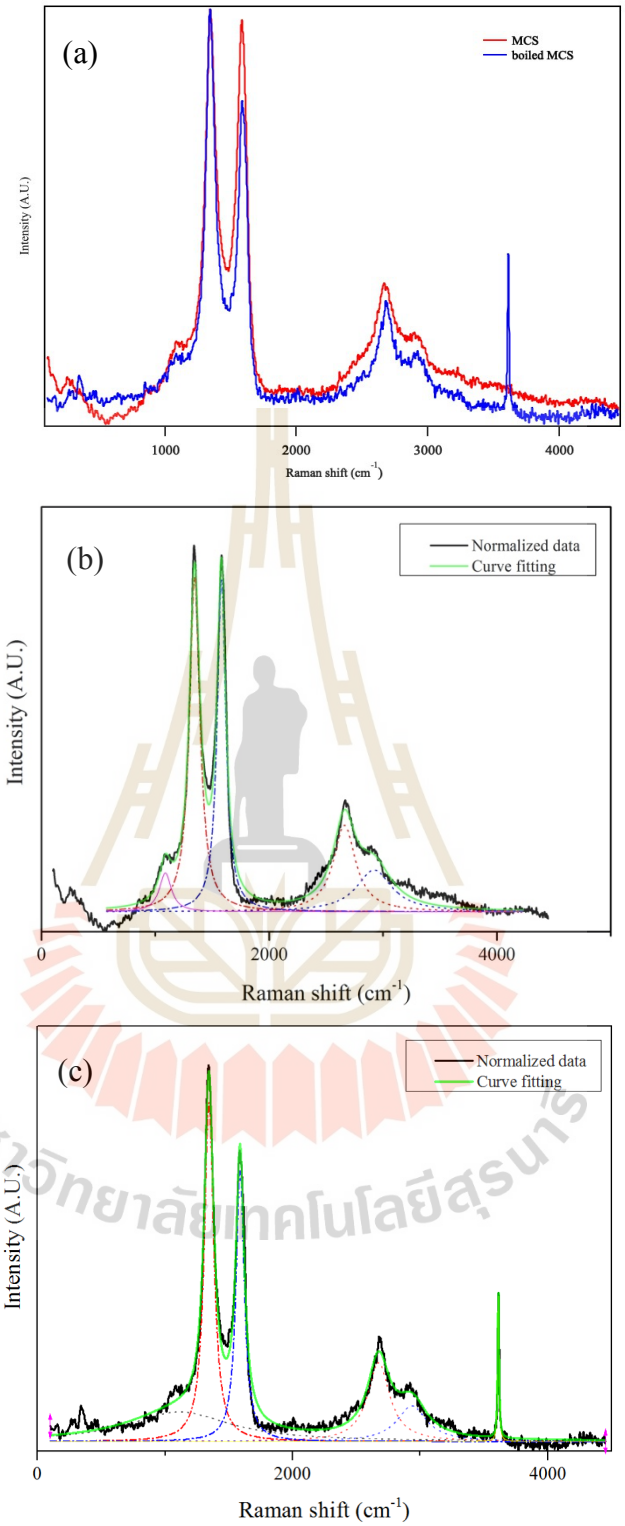

Figure 4.7 (a) Raman spectrum of MCS (red) and boiled MCS (blue). The curve fitting of the Raman spectrum of (b) MCS and (c) boiled MCS.

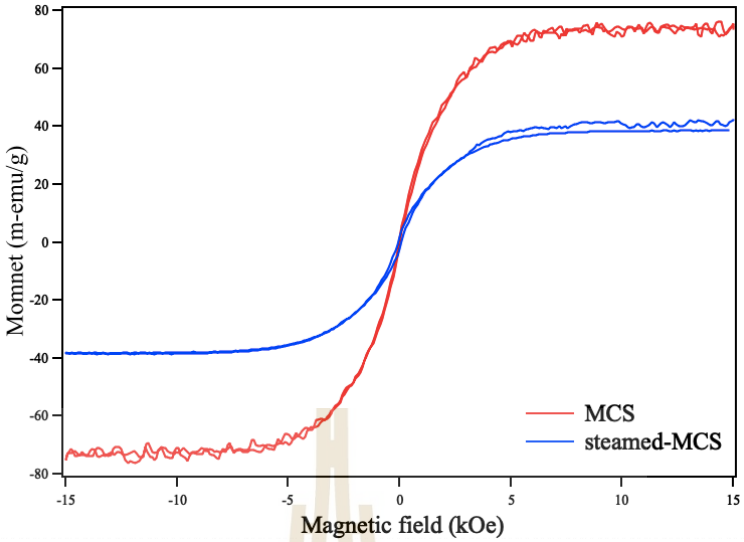

Figure 4.8 Magnetization curve of MCS (a) before and (b) after steam 2 h.

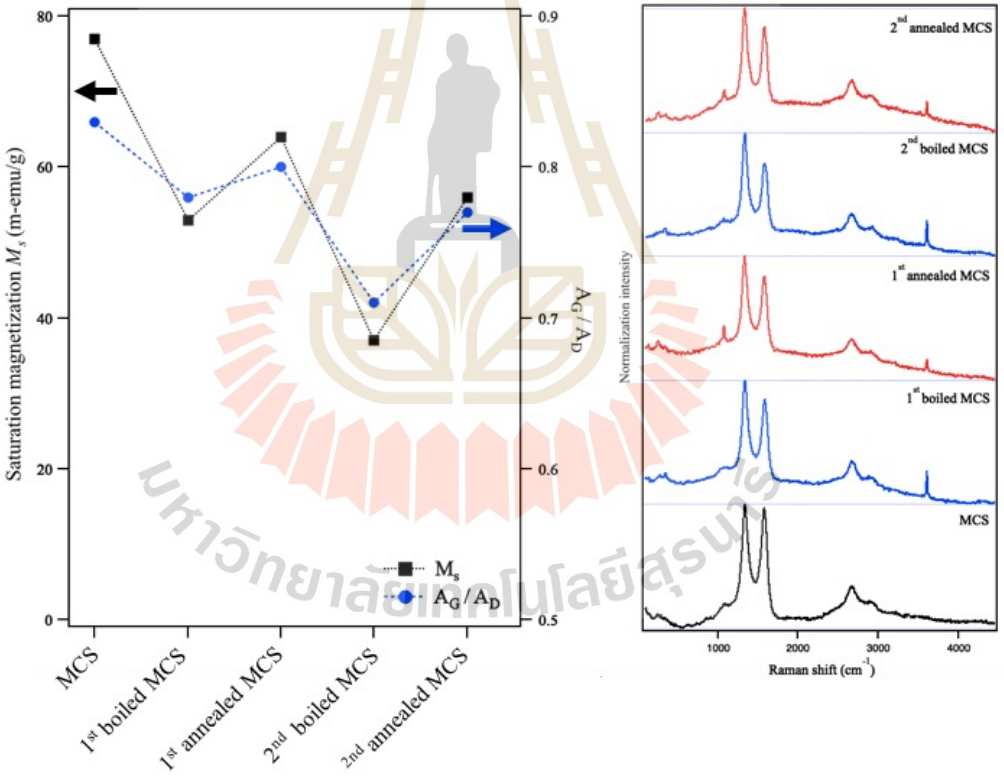

Figure 4.9 (a) the saturation magnetization (M) of MCS after performing by cyclic of boiling in DI water (blue full circle) and annealing in pure Ar (red full-square) at 150 °C for 2 h, the black full-triangle represents MCS. (b) Raman spectrum of MCS after performing by cyclic of boiling in DI water and annealing in pure Ar at 150 °C for 2 h.

CHAPTER V

CONCOUNDTION

5.1 Conclusion of study ferromagnetism in MCS

In conclusion, the ferromagnetic MCS prepared by the chemical vapor deposition (CVD) at 1,050 °C using adamantane as a precursor material exhibits the saturation magnetization of 72 m-emu/g at room temperatures. If we assume that the ferromagnetism occurs only in carbon film, and we calculate the lower-bound value of the saturation magnetization of the only carbon film by knowing that the mass ratio between adamantane precursor and sand particles (0.075) and hence if all the adamantane precursor remains on sand particles after the CVD process, the saturation magnetization is approximate ~1 emu/g. Our Raman spectrum of MCS reveals various carbon bonding, not only sp^3. This feature indicates that the adamantane structure has changed after the CVD process. We assume that the emergence of unpaired electrons or dangling bonds due to carbon bonds was broken during the CVD process.

This magnetic particle is robust where its magnetization still remains 53 m-emu/g (74% of the MCS magnetization) under humidity treatment. The decrease of saturation magnetization could be described by the saturated of unpaired electrons or dangling bonds that are attached to the water. Moreover, the saturation magnetization of MCS can decrease and recover by the cyclic of boiling in DI water and annealing in Ar. After annealing in Ar, the Raman peak of water decreased and increased again after boiled. Raman spectrum reveals the Raman shift of water vapor after boiled MCS. In addition, the boiling process also affects the ratio of G and D peak intensities (A_G/A_D),

this ratio decreased after MCS was boiled and increased after MCS was annealed in Ar. This finding suggests the inexpensive and bio-compatible ways to produce magnetic carbon materials which can be applied in large-scale magnetic shielding and medical treatment applications.

5.2 Future direction

Ferromagnetism in MCS is originated from unpaired electrons or dangling bond due to the intrinsic structural defects. I would like to optimize various parameter, such as mass of precursor, deposition temperature, and pressure in CVD-system for defining strength ferromagnetism in MCS. In medicine, efforts have been made to develop drug delivery within the human body using magnetic nanoparticles. I believe that our MCS will be a way to develop this drug delivery system because it's inexpensive and bio-compatible.

มหาวิทยาลัยเทคโนโลยีสุรนารี

REFERENCES

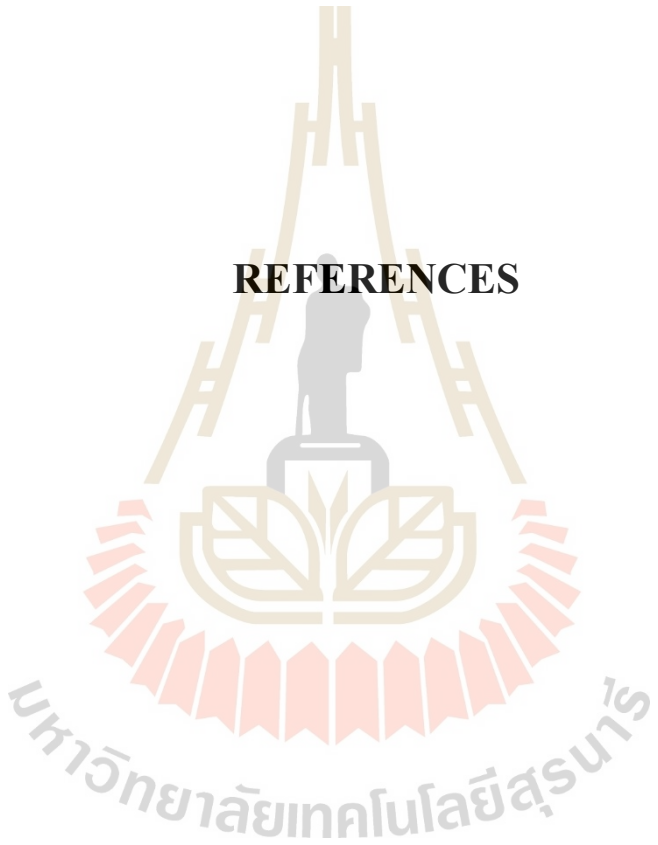

REFERENCES

Andriotis, N., Menon, M., Sheetz, R., and Chernozatonskii, L. (2003). Magnetic properties of C_{60} polymers. **Phys. Rev. Lett.** 90: 26801.

Coey, J. M. D., Venkatesan, M. U. N. U. S. W. A. M. Y., Stamenov, P., Fitzgerald, C. B., and Dorneles, L. S. (2005). Magnetism in hafnium dioxide. **Phys. Rev. B.** 72: 024450. Drummond, N. D. (2007). Nanomaterials: Diamondoids display their potential. **Nat. Nanotechnol.** 2: 462.

Childres, I., Jauregui, L.A., Park, W., Cao, H., and Chen, Y. P. (2013). Raman spectroscopy of graphene and related materials. New developments in photon and materials research. 1: 1-20

Esquinazi, P., Spemann, D., Hohne, R., Setzer, A., Han, K. -H. and Butz, T. (2003). Induced Magnetic Ordering by Proton Irradiation in Graphite. **Phys. Rev. Lett.** 91: 227204

Goldman, A. (1999). Handbook of Modern Ferromagnetic Materials, Kulwer Acad. **Pub, Boston, USA.**

Kim, Y. -H., Choi, J., and Chang, K. J. (2003). Defective fullerenes and nanotubes as molecular magnet: An ab initio study. **Phys. Rev. B**. 68: 12544

Lehtinen, P. O., Foster, A. S., Ma, Y., Krasheninnikov, A. V., and Nieminen, R. M. (2004). Irradiation-induced magnetism in graphite: a density functional study. **Phys. Rev. Lett.** 93: 187202.

มหาวิทยาลัยเทคโนโลยีสุรนารี

Lucchese, M. M., Stavale, F., Ferreira, E. M., Vilani, C., Moutinho, M. V. D. O., Capaz, R. B., Achete, C. A., and Jorio, A. (2010). Quantifying ion-induced defects and Raman relaxation length in graphene. **Carbon**. 48: 1592.

Narasimha, K. T., Ge, C., Fabbri, J. D., Clay, W., Tkachenko, B. A., Fokin, A. A., and Melosh, N. A. (2016). Ultralow effective work function surfaces using diamondoid monolayers. **Nat. Nanotechnol.** 11: 267.

Ma, Y. W., Lu, Y. H., Yi, J. B., Feng, Y. P., Herng, T. S., Liu, X., and Ding, J. (2012). Room temperature ferromagnetism in Teflon due to carbon dangling bonds. **Nat. Commun.** 3: 727.

Meevasana, W., Supruangnet, R., Nakajima, H., Topon, O., Amornkitbamrung, V., and Songsiriritthigul, P. (2009). Electron affinity study of adamantane on Si (1 1 1). **Appl. Surf. Sci.** 256: 934-936.

Mizogami, S., Mizutani, M., Fukuda, M., and Kawabata, K. (1991). Abnormal ferromagnetic behavior for pyrolytic carbon under low temperature growth by CVD method. **Synth. Met**. 43: 3271-3274.

Park, S. H., Kim, Y. G., Kim, D. H., Cheong, H. D., Choi, W. S., and Lee, J. I., (2010). Selecting characteristic Raman wavelengths to distinguish liquid water, water vapor, and ice water. **J. OPT. SOC. KOREA.** 14: 209-214.

Pinitsoontorn, S. (2015). **Magnetic Materials.** Khon Kaen: Khon Kaen University.

Robertson, J. (2002). Diamond-like amorphous carbon. **Mater. Sci. Eng. R Rep.** 37: 129.

Saito, T., Nishio-Hamane, D., Yoshii, S., and Nojima, T. (2011). Ferromagnetic carbon materials prepared from polyacrylonitrile. **Appl. Phys. Lett.** 98: 052506.

Sangphet, S., Siriroj, S., Sriplai, N., Doonyapisut, D., Thila, S., Lowpa, S., and Meevasana, W. (2018). Enhanced ferromagnetism in mechanically exfoliated CVD-carbon films prepared by using adamantane as precursor. **Appl. Phys. Lett.** 112: 242406.

Sriplai, N., Pinitsoontorn, S., Chompoosor, A., Amnuaypanich, S., Maensiri, S., and Amornkitbamrung, V. (2015). Ferromagnetism in metal-free polymers. **IEEE Magn. Lett.** 6: 1-4.

Sundaresan, A., Bhargavi, R., Rangarajan, N., Siddesh, U., and Rao, C. N. R. (2006). Ferromagnetism as a universal feature of nanoparticles of the otherwise nonmagnetic oxides: **Phys. Rev. B.** 74: 161306.

Yang, W. L., Fabbri, J. D., Willey, T. M., Lee, J. R., Dahl J. E., Carlson, R. M. K., Schreiner, P. R., Fokin A. A., Tkachenko, B. A., Fokina, N. A., Meevasana, W., Mannella, N., Tanaka, K., Zhou, X. J., Buuren, T., Kelley, M. A., Hussain, Z., Melosh, N. A., and Shen, Z. -X. (2007). Monochromatic Electron Photoemission from Diamondoid Monolayers. **Science.** 316: 1460-1462

Yu, F., Chen, J., Yang, M., Zhou, L., Jin, L., Su, C., and Ma, J. (2012). A facile one-pot method for synthesis of low-cost magnetic carbon nanotubes and their applications for dye removal. **New J. of Chem.** 36: 1940-1943.

Zanolli, Z., and Charlier, J. C. (2010). Spin transport in carbon nanotubes with magnetic vacancy-defects. **Phys. Rev. B.** 81: 165406.

Zhang, S., Zeng, M., Li, J., Li, J., Xu, J., and Wang, X. (2014). Porous magnetic carbon sheets from biomass as an adsorbent for the fast removal of organic pollutants from aqueous solution. **J. Mater. Chem. A.** 2: 4391-4397.

Zhang, Y., Talapatra, S., Kar, S., Vajtai, R., Nayak, S. K., and Ajayan, P. M. (2007). First-principles study of defect-induced magnetism in carbon. **Phys. Rev. Lett.** 99: 107201.

Zhou, Y., Brittain, A. D., Kong, D., Xiao, M., Meng, Y., and Sun, L. (2015). Derivatization of diamondoids for functional applications. **J. Mater. Chem. C.** 3: 6947-6961.

CURRICULUM VITAE

Name Mr. Yattiphong Kaeokhamchan

Born October 29th, 1994 in Yasothon, Thailand

Citizenship Thai

Address 84 M.2, Tung Tae, Maung, Yasothon, 35000, Thailand

E-mail yattiphong.05@gmail.com

Education

2013-2016 B.Sc. (Physics), Suranaree University of Technology, Thailand

2017-present M.Sc. (Physics), Suranaree University of Technology, Thailand

Oral presentation:

Kaeokhamchan, Y., Sangphet, S., Eknapakul, T., Pinitsoontorn, S., and Meevasana, W. (2019). Synthesis of Magnetic Carbon Sand. Presented at The 2nd Materials Research Society of Thailand International Conference (MRS-Thailand 2019) (2019-07-10 – 2019-07-12).

มหาวิทยาลัยเทคโนโลยีสุรนารี